NASA TECHNICAL NOTE

NASA TN D-2177

NASA TN D-2177

MEASURED TRANSFER FUNCTIONS OF PILOTS DURING TWO-AXIS TASKS WITH MOTION

by Hugh P. Bergeron and James J. Adams

Langley Research Center
Langley Station, Hampton, Va.

NATIONAL AERONAUTICS AND SPACE ADMINISTRATION • WASHINGTON, D. C. • MARCH 1964

MEASURED TRANSFER FUNCTIONS OF PILOTS DURING TWO-AXIS TASKS WITH MOTION

By Hugh P. Bergeron and James J. Adams

Langley Research Center
Langley Station, Hampton, Va.

NATIONAL AERONAUTICS AND SPACE ADMINISTRATION

For sale by the Office of Technical Services, Department of Commerce,
Washington, D.C. 20230 -- Price $1.00

MEASURED TRANSFER FUNCTIONS OF PILOTS DURING TWO-AXIS TASKS WITH MOTION

By Hugh P. Bergeron and James J. Adams

SUMMARY

Measurements of human transfer functions, made by matching an analog pilot to a human pilot, have been obtained in tests where the variables were the number of axes being controlled, and operation with and without cockpit angular motion corresponding to the indicated error. The analog pilot contained three gains which were automatically adjusted to match the pilot. The tests were made with a gimbal-mounted simulator in which the simulated dynamics represented an inertia system with linear damping and control $2/s(s + 1)$ where s is the Laplace transform.

The results show that although a pilot operates in a manner similar to a linear mechanism with constant gains when in a fixed-base, single-axis control loop, the addition of a second axis to his task causes him to operate with time-varying gains. The further addition of motion to the simulation greatly reduces the amount of time variation in the measured gains of the pilot. The tests show that the measuring method promises to be a very useful means for obtaining data on human characteristics.

INTRODUCTION

Investigations of human transfer functions in previous studies (refs. 1 to 7) have been concerned mostly with fixed-base single-degree-of-freedom simulations. Although this type of investigation is necessary to obtain a good background from which to work, it does not realistically represent normal human operation in various craft. This study represents an attempt to investigate the effect of multiaxis tasks, with and without motion cues, on the characteristics of a human transfer function.

The transfer functions were obtained by using an automatic model-matching technique. (See refs. 1 and 2.) Although visual cues are considered to be the principal basis for pilot control, motion cues may have an effect on the control of vehicles in which motion cues can be readily detected. Multiple-axis operation is important in that it represents a more realistic job; that is, under normal conditions, a pilot will usually have to perform two or more operations simultaneously. In the present investigation one- and then two-axis tasks, in that order, were mechanized. The simulator used in these tests was a gimbal-mounted moving cockpit.

It is felt that an evaluation of the data presented may help engineers in assigning pilot tasks and in determining pilot requirements. This paper should also prompt investigators to probe these factors and their bearing on human transfer functions further.

SYMBOLS

D	disturbance input, volts
K_1, K_2	gains
s	Laplace transform
ϵ_1	roll-axis displayed error, volts or deg
ϵ_2	pitch-axis displayed error, volts or deg
δ_{11}	output of analog pilot in roll axis, volts
δ_{22}	output of analog pilot in pitch axis, volts
δ_1	pilot output in roll axis, volts
δ_2	pilot output in pitch axis, volts
ϕ	controlled dynamics output in roll axis, volts
θ	controlled dynamics output in pitch axis, volts
ω	frequency of pilot-vehicle characteristic equation, radians/sec
ρ	damping ratio of pilot-vehicle characteristic equation
τ	lag frequency break point, radians/sec

DESCRIPTION AND OPERATION OF THE SIMULATOR

This paper is an extension of previous work as reported in references 1 and 2. In particular, this report represents an analysis of data obtained from one- and two-axis simulations with and without motion cues. The task presented to the pilots was a compensatory one, that is, one in which an indicator was to be alined with a fixed reference. The model of the transfer function and the automatic matching technique utilized are derived and explained in reference 2. Figure 1 shows a block diagram of the test equipment for one axis. The automatic adjusting feature of the analog pilot is shown for one of the gains. The other two gains work in a similar manner. The filters for each of the gains are derived

in reference 2 along with a computer diagram representing the model of the transfer function and its automatic adjusting feature.

The pilot operated through a dynamics of $2/s(s + 1)$. (See sketch.) (The error signal consisted of the pilot's control signal having gone through the

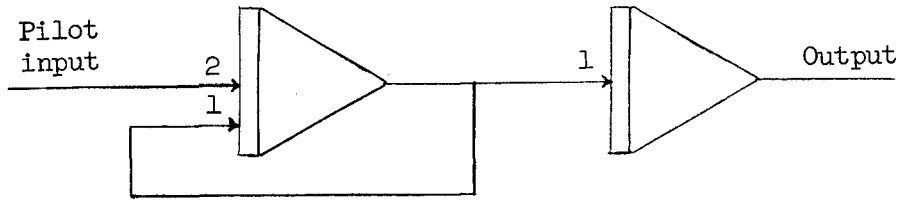

dynamics $2/s(s + 1)$ plus the disturbance signal.) (See fig. 2.) In the present investigation, input and output data were recorded on magnetic tape. By using magnetic tape the matching technique could be optimized by reusing this raw data. A photograph of the simulator is shown in figure 3. The visual reference cues were obtained from an 8-ball mounted in the center of the instrument panel. (See fig. 4.) To assure that the pilots did not receive visual cues from outside the cockpit during the motion runs, the simulator was operated in a surrounding of complete darkness. Only the instruments on the panel were lighted. The diameter of the face of the 8-ball was $4\frac{1}{2}$ inches and it was located approximately 20 to 24 inches from the observer. Control was imparted to the vehicle through a side-arm controller (see fig. 4), the arm of which was 3 inches high. Light centering springs were utilized in the two degrees of freedom of the controller. In the experiment, fore-and-aft movement of the controller controlled the pitch of the vehicle and 8-ball in the motion and no-motion simulations. Side-to-side movement controlled the yaw of the 8-ball in the no-motion simulations and the roll of the vehicle and 8-ball in the motion runs. The use of the yaw axis instead of the roll axis in the no-motion runs was necessary because of the wiring of the simulator. To eliminate redundancy, side-to-side movement of the controller will always be referred to as the roll axis of the simulator.

The side-arm controller had a freedom of movement of $\pm 30^\circ$ in both the pitch- and roll-axis control. The output of the controller for maximum deflection in the pitch axis was ± 24.5 volts. Therefore, its output was 0.817 volt per degree of stick movement. The output for maximum deflection in the roll axis was ± 31 volts; therefore, its output was 1.032 volts per degree of stick movement.

A step input of 1° from the side-arm controller in the pitch axis imparted a maximum acceleration of 5.88° per second^2 to the vehicle. The corresponding maximum velocity was 5.88° per second. A similar input into the roll axis imparted a maximum acceleration of 4.14° per second^2, and a maximum velocity of 4.14° per second. These vehicle characteristics are considered to be in a satisfactory range of control. The data show the error signal in degrees. The pilot's control signal is shown in volts so that it can be related to the analog pilot signal. The angle the controller moved in degrees, that is, the pilot's control signal in degrees, can be easily determined from the preceding information. The error signal corresponds to the angle which the 8-ball rotated through in the no-motion runs. In the motion runs the vehicle moved through an angle represented

by the error signal and the attitude of the 8-ball remained fixed in inertial space. The vehicle was controlled and moved by hydraulic pressure. The frequency response of the simulator was flat to 9.42 radians per second. Subsequent analysis determined that the natural frequency of the pilot-controlled system was 3.5 radians per second; this value is well within the response of the simulator. The disturbance signal (forcing function) consisted of a Gaussian noise generator which was filtered with two first-order filters to a noise break frequency of 0.25 radian per second. This signal was fed to the vehicle on the path represented in the flow diagram shown in figure 2. This is the disturbance signal recorded on the recorder and is used in obtaining the error. This error signal is the signal recorded for vehicle and 8-ball error.

The same disturbance signal was used for both the pitch and roll axes when both axes were in operation. However, examination of the error signals of the pitch and roll axes during a typical run (see 2-axis runs for pilot A with no motion) shows no correlation between the two signals when they were plotted against each other on an X,Y plotter. (See fig. 5.) Also, the pilots remarked that they were unable to detect any similarity between the correction signals required for the two axes. This condition is probably due partly to the fact that as soon as different correction signals are applied to the simulator, the error signals will correspondingly differ and in continual operation this difference will be a random function.

Before each recorded run the pilot was given a short practice run. The first task required of the pilots was to control a single-degree-of-freedom simulation with no motion. (Note that the pitch axis was used for all single-degree-of-freedom simulations.) For his second task, motion was added to the pitch axis. In all motion runs, the pilot was strapped down in the cockpit. The third task was that of controlling two axes without motion. For his fourth and final task, motion was added to both axes. The pilot knew at all times which runs were considered practice and which were considered data runs. As the raw data were being recorded on magnetic tape, an analog pilot fit was simultaneously being conducted.

All pilots were in general agreement that the difficulty of the task was high. However, they all maintained reasonable control inasmuch as they were able to keep the error signal smaller than the disturbance or uncontrolled signal.

INVESTIGATION OF THE ANALOG-PILOT AUTOMATIC-GAIN-CORRECTION FEATURE

To obtain a calibration of the automatic-gain-adjustment feature of the model analog pilot, several runs were made in which a sine wave of set frequency was applied to one of the gains on a second analog pilot. The other gains of the second analog pilot were kept constant. This analog pilot was then inserted into the computer program in place of the pilot as is seen in figure 6. The model analog pilot was required to follow the second analog pilot. The K_2, τ, and K_1 in figures 7 to 10 are the gains of the model analog pilot. The sine wave at the bottom of each figure is the sine wave form inserted for the particular gain in the second analog pilot.

MEASURED TRANSFER FUNCTIONS OF PILOTS DURING TWO-AXIS TASKS WITH MOTION

By Hugh P. Bergeron and James J. Adams

SUMMARY

Measurements of human transfer functions, made by matching an analog pilot to a human pilot, have been obtained in tests where the variables were the number of axes being controlled, and operation with and without cockpit angular motion corresponding to the indicated error. The analog pilot contained three gains which were automatically adjusted to match the pilot. The tests were made with a gimbal-mounted simulator in which the simulated dynamics represented an inertia system with linear damping and control $2/s(s + 1)$ where s is the Laplace transform.

The results show that although a pilot operates in a manner similar to a linear mechanism with constant gains when in a fixed-base, single-axis control loop, the addition of a second axis to his task causes him to operate with time-varying gains. The further addition of motion to the simulation greatly reduces the amount of time variation in the measured gains of the pilot. The tests show that the measuring method promises to be a very useful means for obtaining data on human characteristics.

INTRODUCTION

Investigations of human transfer functions in previous studies (refs. 1 to 7) have been concerned mostly with fixed-base single-degree-of-freedom simulations. Although this type of investigation is necessary to obtain a good background from which to work, it does not realistically represent normal human operation in various craft. This study represents an attempt to investigate the effect of multiaxis tasks, with and without motion cues, on the characteristics of a human transfer function.

The transfer functions were obtained by using an automatic model-matching technique. (See refs. 1 and 2.) Although visual cues are considered to be the principal basis for pilot control, motion cues may have an effect on the control of vehicles in which motion cues can be readily detected. Multiple-axis operation is important in that it represents a more realistic job; that is, under normal conditions, a pilot will usually have to perform two or more operations simultaneously. In the present investigation one- and then two-axis tasks, in that order, were mechanized. The simulator used in these tests was a gimbal-mounted moving cockpit.

It is felt t
assigning pilot t
also prompt inves
transfer function

D	disturt
K_1, K_2	gains
s	Laplace
ϵ_1	roll-a>
ϵ_2	pitch-ε
δ_{11}	output
δ_{22}	output
δ_1	pilot (
δ_2	pilot (
ϕ	contro.
θ	contro.
ω	freque
ρ	dampin
τ	lag fr

by the error signal and the attitude of the 8-ball remained fixed in inertial space. The vehicle was controlled and moved by hydraulic pressure. The frequency response of the simulator was flat to 9.42 radians per second. Subsequent analysis determined that the natural frequency of the pilot-controlled system was 3.5 radians per second; this value is well within the response of the simulator. The disturbance signal (forcing function) consisted of a Gaussian noise generator which was filtered with two first-order filters to a noise break frequency of 0.25 radian per second. This signal was fed to the vehicle on the path represented in the flow diagram shown in figure 2. This is the disturbance signal recorded on the recorder and is used in obtaining the error. This error signal is the signal recorded for vehicle and 8-ball error.

The same disturbance signal was used for both the pitch and roll axes when both axes were in operation. However, examination of the error signals of the pitch and roll axes during a typical run (see 2-axis runs for pilot A with no motion) shows no correlation between the two signals when they were plotted against each other on an X,Y plotter. (See fig. 5.) Also, the pilots remarked that they were unable to detect any similarity between the correction signals required for the two axes. This condition is probably due partly to the fact that as soon as different correction signals are applied to the simulator, the error signals will correspondingly differ and in continual operation this difference will be a random function.

Before each recorded run the pilot was given a short practice run. The first task required of the pilots was to control a single-degree-of-freedom simulation with no motion. (Note that the pitch axis was used for all single-degree-of-freedom simulations.) For his second task, motion was added to the pitch axis. In all motion runs, the pilot was strapped down in the cockpit. The third task was that of controlling two axes without motion. For his fourth and final task, motion was added to both axes. The pilot knew at all times which runs were considered practice and which were considered data runs. As the raw data were being recorded on magnetic tape, an analog pilot fit was simultaneously being conducted

All pilots were in general agreement that the difficulty of the task was high. However, they all maintained reasonable control inasmuch as they were able to keep the error signal smaller than the disturbance or uncontrolled signal.

INVESTIGATION OF THE ANALOG-PILOT AUTOMATIC-GAIN-CORRECTION FEATURE

This paper
and 2. In parti
one- and two-axi
to the pilots wa
be alined with a
automatic matchi
Figure 1 shows a
adjusting featur
two gains work i

To obtain a calibration of the automatic-gain-adjustment feature of the model analog pilot, several runs were made in which a sine wave of set frequency was applied to one of the gains on a second analog pilot. The other gains of the second analog pilot were kept constant. This analog pilot was then inserted into the computer program in place of the pilot as is seen in figure 6. The model analog pilot was required to follow the second analog pilot. The K_2, τ, and K_1 in figures 7 to 10 are the gains of the model analog pilot. The sine wave at the bottom of each figure is the sine wave form inserted for the particular gain in the second analog pilot.

The error signal used in these runs consisted of the sum of the disturbance signal and the pilot (in this case the second analog pilot) output signal through the dynamics. The disturbance signal or forcing function was a filtered signal from a Gaussian noise generator with a break frequency of 1 radian per second. The operating dynamics was $2/s(s + 1)$. Several tests were made in which each gain of the second analog pilot was individually varied by various sine wave functions of constant frequency. During these runs the other gains were kept constant in order to determine the frequency response of the individual gain adjustment filters and the interaction that the adjustment of one of the gains caused on the other two gains. The gains for four of these runs are illustrated in figures 7 to 10.

Figures 7, 9, and 10 show the highest frequency to which the individual gains could adjust without decreasing significantly in amplitude. Figure 7 illustrates the response of the K_2 gain. The frequency of the sine wave input was 0.3 cycle per second. The reason for there being variations in the amplitude of the K_2 gain can be attributed to two factors. (1) For K_2 to adjust to a new value, the difference between the pilot and analog pilot must be a large enough value. This difference is directly dependent on the amplitude of the error signal. If the difference happens to be small when the programed K_2 gain is different from the model analog pilot K_2 gain, little or no adjustment will take place. (2) The gain must need adjusting; that is, even though the difference is large, little or no adjustment will take place if the programed K_2 gain is near the model analog pilot K_2 gain. This logic holds for the K_1 and τ gains also. Figure 8 demonstrates this effect more vividly by the use of a sine-wave input of high frequency (1 cycle/second) for K_2.

The K_1 gain (see fig. 9) does not respond as rapidly as the K_2 gain. Also, some interaction is evident on both the K_2 and τ gains. The sine-wave input in this case was made at 0.06 cycle per second. The results of the τ gain illustrated in figure 10 closely resemble that of the K_1 gain. These results were obtained with a frequency of 0.06 cycle per second.

RESULTS AND DISCUSSION

The data presented consist of one- and two-axis simulations with and without motion cues. Figures 11 to 26 represent the runs for three pilots through the complete task schedule. The pilots are designated by the same letter reference as in reference 2; that is, pilot A in reference 2 is pilot A in this report.

It is significant that in performing all the different tasks the pilots maintained an average calculated frequency and damping ratio that agreed with previous data taken on similar tasks of equal difficulty. It should be emphasized, however, that these values constitute the average of a complete run. Further investigation of the time histories indicated certain specific variations between the various tasks.

Figures 11, 12, and 13 represent single-axis tasks without motion for pilots A, B, and D, respectively, and present the error, pilot, analog pilot, and gain signals. In addition, a typical disturbance signal is displayed on figure 11. Figure 14 represents a single-axis task with motion for pilot A. Since there were normally only minor variations in the time histories of this task and the previous task, only one time history was displayed. It can be seen, however, in this particular run that the pilot operated with a fairly high frequency. This run, however, was the first performed by this pilot with motion and his frequency dropped in subsequent runs in which he operated with motion cues.

The next task consisted of two-axis operation without motion. Figures 15 and 16(a) present records of the two-axis runs made by pilot A. One must remember that in all the two-axis runs, both axes for each task were controlled at the same time, that is, the runs shown in figures 15 and 16(a) were performed at the same time, that in figure 15 corresponding to the pitch axis and that in figure 16(a) to the roll axis. All the gains K_1, τ, and K_2, for these two-axis runs show a definite change from that shown in figure 11 in that they vary considerably during the run. Also, the error signals are larger in the runs shown in figures 15 and 16(a). Note in particular the spikes in K_1 of the two-axis runs and see how they correspond to the large error displays. Figures 16(b), 16(c), and 16(d) represent the gains obtained from re-runs of the task performed in figure 16(a). These re-runs were accomplished by using data stored on magnetic tape. The object was to investigate each gain individually to determine the accuracy of the results obtained in figure 16(a), the run in which all three gains were computed at the same time. The scaling of the gains in figures 16(b), 16(c), and 16(d) is twice that of the gains in figure 16(a). Figure 16(a) also had its gains inverted with respect to the other three figures. When the data in figure 16(a) were run, the computer became unstable about three-fourths of the way through the run. In later tests with the same data, the entire run was completed. The arrows at the top of figures 16(b), 16(c), and 16(d) designate the location where the run became unstable in figure 16(a).

In the re-runs two of the gains were kept fairly constant by lowering the gain in the automatic-gain adjustment loops. It was felt that if keeping two of the gains constant did not increase the measured variations in the third gain, greater confidence could be placed in the measured variations. It can be seen in the re-runs that only slight variations from the time histories of the gains presented in figure 16(a) exist. It is concluded that the measured variations in gain do accurately reflect gain variations present in the pilot, and these variations are due only in a small part to the type of interaction shown in the calibrations presented in figures 7 to 10. Figures 17 and 18 show records made by pilot B. Again a definite change is noted in the gains and error signals. The spiked variations in K_1 are more pronounced in figure 18 than in the previously mentioned two-axis runs. Again, these spikes can be related to large variations in the error signal. In the third pilot's runs (figs. 19 and 20), changed gains and error signals as related to the pilot's single-axis run (fig. 13) can again be seen. As noted in figure 19 the values of K_1 and τ gains were initially set too far from their final value and, as can be seen, never did reach this steady-state value. For this reason the values of K_1 and τ had to decrease continually and a variation from the steady-state average would

not be as readily noticed. However, the run shown in figure 20 typifies previous results and large variations of the gains are evident.

The final task presented to each pilot involved two-axis control with cockpit motion present in the simulation. The runs shown in figures 21 and 22 are the pitch and roll time histories with pilot A; the runs in figures 23 and 24, for pilot B; and the runs in figures 25 and 26, for pilot D. In all these runs the measured gains show very little variation with time when compared with the two-axis tests without motion. Also, the error does not contain the larger excursions noted in the runs without motion. A possible explanation of the effects noted when motion was added to the simulation is as follows. When a pilot is controlling two axes, he may at times neglect the visual presentation for one axis while he concentrates on controlling the other axis. If the visual cue is the pilot's only cue, there will be times during which no control will be exercised on the neglected axis. If the pilot also has a motion cue, he will use this motion cue during the times that he is neglecting the visual cue to aid him in maintaining a constant level of control.

Table I represents a listing of data obtained from each pilot. The various tasks are grouped in the following order: The first task is a single-axis simulation without motion. This task is followed by a single-axis simulation with motion. The third task consists of a two-axis simulation without motion. Because of the large variations in the K_2 gain, three groups of data are listed as representing this task. A minimum, average, and maximum value of K_2 are considered. The fourth, and final, task represents a two-axis simulation with motion. The data listed consist of the measured gains, the calculated transfer function of the pilot, and the closed-loop characteristics. The transfer function of the pilot is in the form:

$$\frac{\frac{K_1}{\tau}\left(1 + \frac{K_2}{\tau}\right)s}{\left(1 + \frac{1}{\tau}s\right)^2}$$

The closed-loop (θ/D or ϕ/D) characteristics represent the output of the complete system over the disturbance.

The calculated closed-loop characteristics show that using the average values of the measured gains for the pilot results in frequencies, damping ratios, and real roots that are very nearly the same for all the tests. The one exception is the high damping ratio obtained with pilot D on the roll axis. The results also agree closely with the results obtained in reference 2 with the same controlled dynamics, the exception being that the real roots obtained in the present investigation are lower.

In addition to using the average measured values of the gains, the maximum and minimum measured values of K_2 measured in the two-axis tests without motion were used in conjunction with the average values of K_1 and τ in calculating closed-loop characteristics. In general, these calculations show that the closed-loop damping ratios are less with the maximum and minimum values of K_2 than were

those obtained with the average values. In some cases the use of the minimum value of K_2 caused the real roots to combine to form a complex root with damping less than 1 and the original complex root to have a negative damping ratio. The exception to this general trend is the pitch axis with pilot A, in which the minimum value of K_2 resulted in a higher damping ratio than the average value. There are also instances during the tests when K_1 dropped to a low or zero value, and thus indicated that no control was being exercised.

CONCLUDING REMARKS

The present investigation indicates that although a pilot operates in a manner similar to a linear mechanism with constant gains when in a fixed-base simulated single-axis control loop, the addition of a second axis to his control task causes him to operate with time-varying gains. The further addition of angular motion corresponding to the indicated error to the simulation greatly reduced the amount of time variation in the measured gains of the pilot.

The quantitative values obtained in these tests must be viewed with caution in view of the amount of interaction and the slow response shown in the frequency-response calibration of the measuring method. However, these preliminary tests show that the method promises to be very useful in obtaining data on human characteristics.

Langley Research Center,
National Aeronautics and Space Administration,
Langley Station, Hampton, Va., October 15, 1963.

REFERENCES

1. Adams, James J.: A Simplified Method for Measuring Human Transfer Functions. NASA TN D-1782, 1963.

2. Adams, James J., and Bergeron, Hugh P.: Measured Variation in the Transfer Function of a Human Pilot in Single-Axis Tasks. NASA TN D-1952, 1963.

3. Kuehnel, Helmut A.: Human Pilots' Dynamic-Response Characteristics Measured in Flight and on a Nonmoving Simulator. NASA TN D-1229, 1962.

4. Hall, Ian A. M.: Effects of Controlled Element on the Human Pilot. WADC Tech. Rep. 57-509 (ASTIA Doc. No. AD 130979), U.S. Air Force, Aug. 1958.

5. McRuer, Duane T., and Krendel, Ezra S.: The Human Operator as a Servo System Element. Jour. Franklin Inst.
   Pt. I, vol. 267, no. 5, May 1959, pp. 381-403.
   Pt. II, vol. 267, no. 6, June 1959, pp. 511-536.

6. Seckel, Edward, Hall, Ian A. M., McRuer, Duane T., and Weir, David H.: Human Pilot Dynamic Response in Flight and Simulator. WADC Tech. Rep. 57-520, ASTIA Doc. No. AD 130988, U.S. Air Force, Aug. 1958.

7. Elkind, Jerome I.: Characteristics of Simple Manual Control Systems. Tech. Rep. No. 111, Lincoln Lab., M.I.T., April 6, 1956.

TABLE I.- MEASURED AND CALCULATED VALUES FROM PILOT TESTS

(a) Pilot A

Task	Type of run	Measured gains			Transfer function, $\frac{K_1}{\tau}\left(1 + \frac{K_2}{\tau}s\right) \Big/ \left(1 + \frac{1}{\tau}s\right)^2$	Closed-loop characteristics		
		K_1	τ	K_2		ω	ρ	Real roots
1	Pitch axis only; without motion	6.5	5	5.5	$\frac{1.3(1 + 1.1s)}{(1 + 0.2s)^2}$	3.029	0.348	-8.007; -0.885
2	Pitch axis only; with motion	12	5	6	$\frac{2.4(1 + 1.2s)}{(1 + 0.2s)^2}$	4.037	.143	-9.034; -0.815
3(a)	Pitch and roll axis; pitch axis without motion; maximum K_2	6.5	5	10	$\frac{1.3(1 + 2s)}{(1 + 0.2s)^2}$	3.97	.202	-8.93; -0.461
3(a)	Pitch and roll axis; roll axis without motion; maximum K_2	10	5	9	$\frac{2(1 + 1.8s)}{(1 + 0.2s)^2}$	4.47	.112	-9.47; -0.528
3(b)	Pitch and roll axis; pitch axis without motion; average K_2	6.5	5	7	$\frac{1.3(1 + 1.4s)}{(1 + 0.2s)^2}$	3.41	.289	-8.362; -0.669
3(b)	Pitch and roll axis; roll axis without motion; average K_2	10	5	5	$\frac{2(1 + s)}{(1 + 0.2s)^2}$	3.442	.226	-8.442; -1.00
3(c)	Pitch and roll axis; pitch axis without motion; minimum K_2	6.5	5	5	$\frac{1.3(1 + s)}{(1 + 0.2s)^2}$	2.87	.370	-7.87; -1.00
3(c)	Pitch and roll axis; roll axis without motion; minimum K_2	10	5	0	$\frac{2(1 + 0s)}{(1 + 0.2s)^2}$	5.876 1.702	.954 -.0636	
4	Pitch and roll axis; pitch axis with motion	6.5	4.5	7	$\frac{1.44(1 + 1.56s)}{(1 + 0.222s)^2}$	3.49	.205	-7.966; -0.603
4	Pitch and roll axis; roll axis with motion	9	4	2.5	$\frac{2.25(1 + 0.625s)}{(1 + 0.25s)^2}$	2.521	.152	-6.486; -1.747

TABLE I.- MEASURED AND CALCULATED VALUES FROM PILOT TESTS - Continued

(b) Pilot B

Task	Type of run	Measured gains			Transfer function, $\frac{K_1}{\tau}\left(1 + \frac{K_2}{\tau} s\right) \Big/ \left(1 + \frac{1}{\tau} s\right)^2$	Closed-loop characteristics		
		K_1	τ	K_2		ω	ρ	Real roots
1	Pitch axis only; without motion	8	4	6	$\frac{2(1 + 1.5s)}{(1 + 0.25s)^2}$	3.621	0.1	-7.634; -0.640
2	Pitch axis only; with motion	7	3.5	3	$\frac{2(1 + 0.857s)}{(1 + 0.285s)^2}$	2.595	.139	-6.084; -1.196
3(a)	Pitch and roll axis; pitch axis without motion; maximum K_2	9	5	6	$\frac{1.8(1 + 1.2s)}{(1 + 0.2s)^2}$	3.59	.224	-8.58; -0.808
3(a)	Pitch and roll axis; roll axis without motion; maximum K_2	9	5	8	$\frac{1.8(1 + 1.6s)}{(1 + 0.2s)^2}$	4.092	.1628	-9.07; -0.592
3(b)	Pitch and roll axis; pitch axis without motion; average K_2	9	5	4	$\frac{1.8(1 + 0.8s)}{(1 + 0.2s)^2}$	2.914	.294	-7.954; -1.333
3(b)	Pitch and roll axis; roll axis without motion; average K_2	9	5	3	$\frac{1.8(1 + 0.6s)}{(1 + 0.2s)^2}$	2.444	.299	-7.537; -2.000
3(c)	Pitch and roll axis; pitch axis without motion; minimum K_2	9	5	1	$\frac{1.8(1 + 0.2s)}{(1 + 0.2s)^2}$	1.78	.0905	-5.678; -5.0
3(c)	Pitch and roll axis; roll axis without motion; minimum K_2	9	5	0	$\frac{1.8(1 + 0s)}{(1 + 0.2s)^2}$	5.819 6.99	.957 -.972	
4	Pitch and roll axis; pitch axis with motion	8	5	5	$\frac{1.6(1 + s)}{(1 + 0.2s)^2}$	3.136	.297	-8.136; -1.000
4	Pitch and roll axis; roll axis with motion	6	3.5	2.5	$\frac{1.715(1 + 0.715s)}{(1 + 0.288s)^2}$	2.217	.182	-5.695; -1.5

TABLE I.- MEASURED AND CALCULATED VALUES FROM PILOT TESTS - Concluded

(c) Pilot D

Task	Type of run	Measured gains			Transfer function, $\frac{K_1}{\tau}\left(1 + \frac{K_2}{\tau}s\right) \Big/ \left(1 + \frac{1}{\tau}s\right)^2$	Closed-loop characteristics		
		K_1	τ	K_2		ω	ρ	Real roots
1	Pitch axis only; without motion	8	4	5	$\frac{2(1 + 1.25s)}{(1 + 0.25s)^2}$	3.346	0.130	-7.351; -0.778
2	Pitch axis only; with motion	7	4	5	$\frac{1.75(1 + 1.25s)}{(1 + 0.25s)^2}$	3.176	.166	-7.174; -0.774
3(a)	Pitch and roll axis; pitch axis without motion; maximum K_2	4.5	3	6	$\frac{1.5(1 + 2s)}{(1 + 0.33s)^2}$	3.064	.0678	-6.114; -0.47
3(a)	Pitch and roll axis; roll axis without motion; maximum K_2	3	7	16	$\frac{0.44(1 + 2.3s)}{(1 + 0.143s)^2}$	3.51	.64	-10.17; -0.334
3(b)	Pitch and roll axis; pitch axis without motion; average K_2	4.5	3	3	$\frac{1.5(1 + s)}{(1 + 0.33s)^2}$	2.265	.162	-5.265; -1.000
3(b)	Pitch and roll axis; roll axis without motion; average K_2	3	7	10	$\frac{0.44(1 + 1.43s)}{(1 + 0.143s)^2}$	2.892	.852	-9.55; -0.526
3(c)	Pitch and roll axis; pitch axis without motion; minimum K_2	4.5	3	0	$\frac{1.5(1 + 0s)}{(1 + 0.33s)^2}$	3.888 1.336	.9338 -.0982	
3(c)	Pitch and roll axis; roll axis without motion; minimum K_2	3	7	4	$\frac{0.44(1 + 0.57s)}{(1 + 0.143s)^2}$	.986	.702	-8.59; -5.03
4	Pitch and roll axis; pitch axis with motion	8	5	5	$\frac{1.6(1 + s)}{(1 + 0.2s)^2}$	3.136	.297	-8.136; -1.00
4	Pitch and roll axis; roll axis with motion	5	4	3	$\frac{1.25(1 + 0.75s)}{(1 + 0.25s)^2}$	2.095	.329	-6.138; -1.485

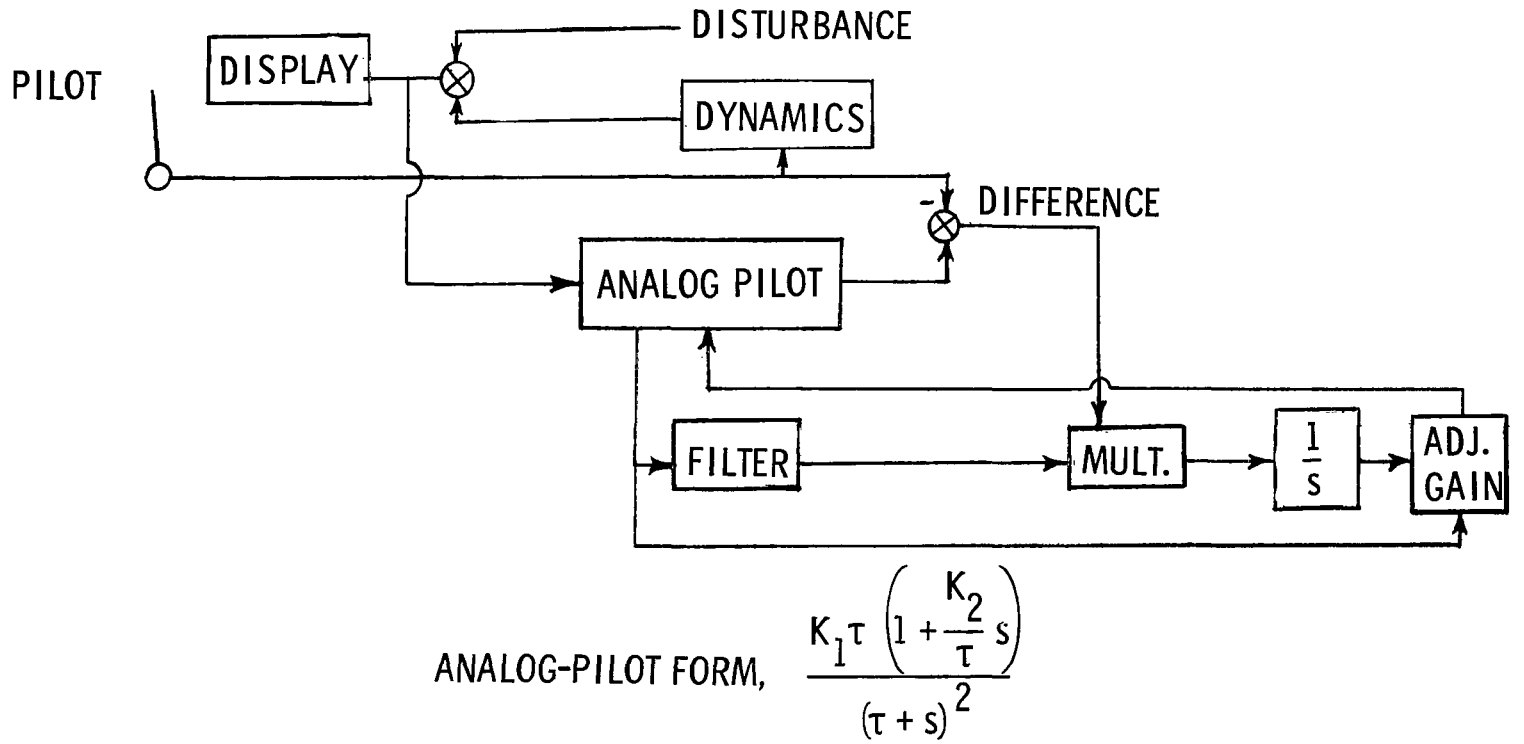

Figure 1.- Block diagram of test equipment.

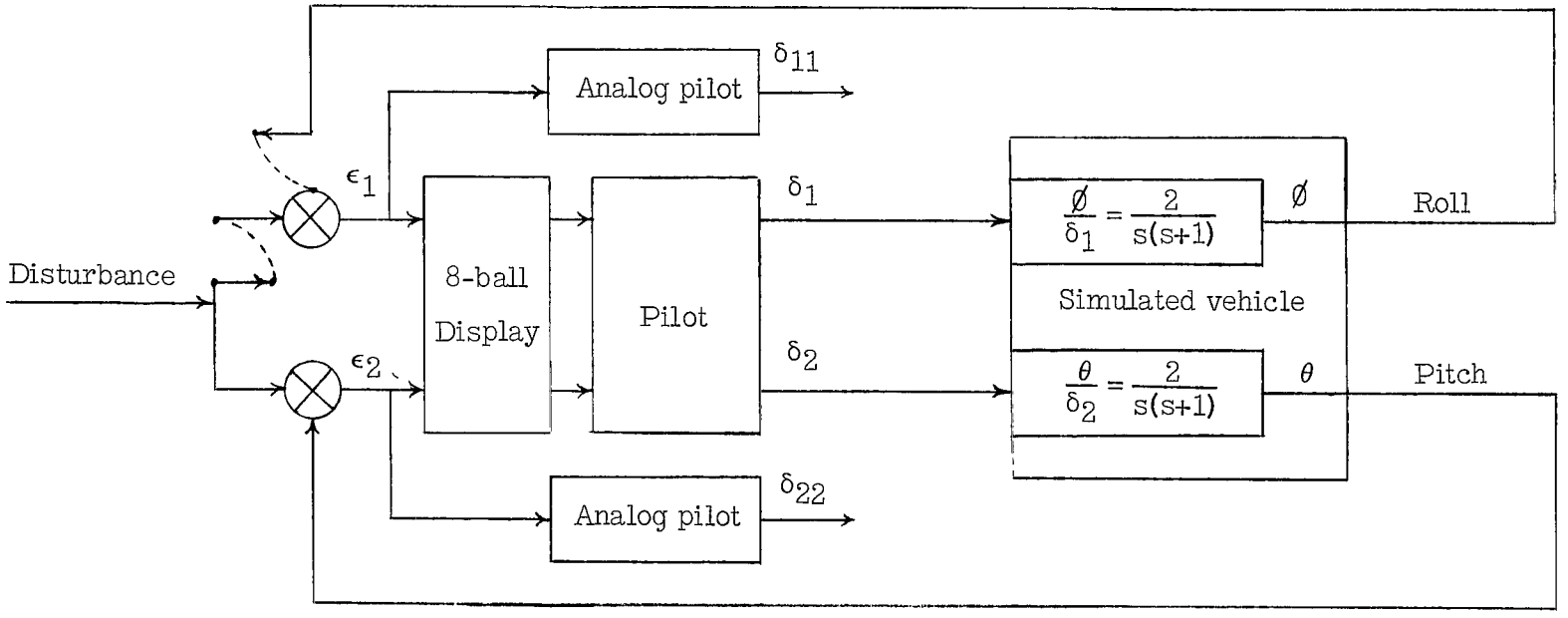

Figure 2.- Flow diagram of simulation.

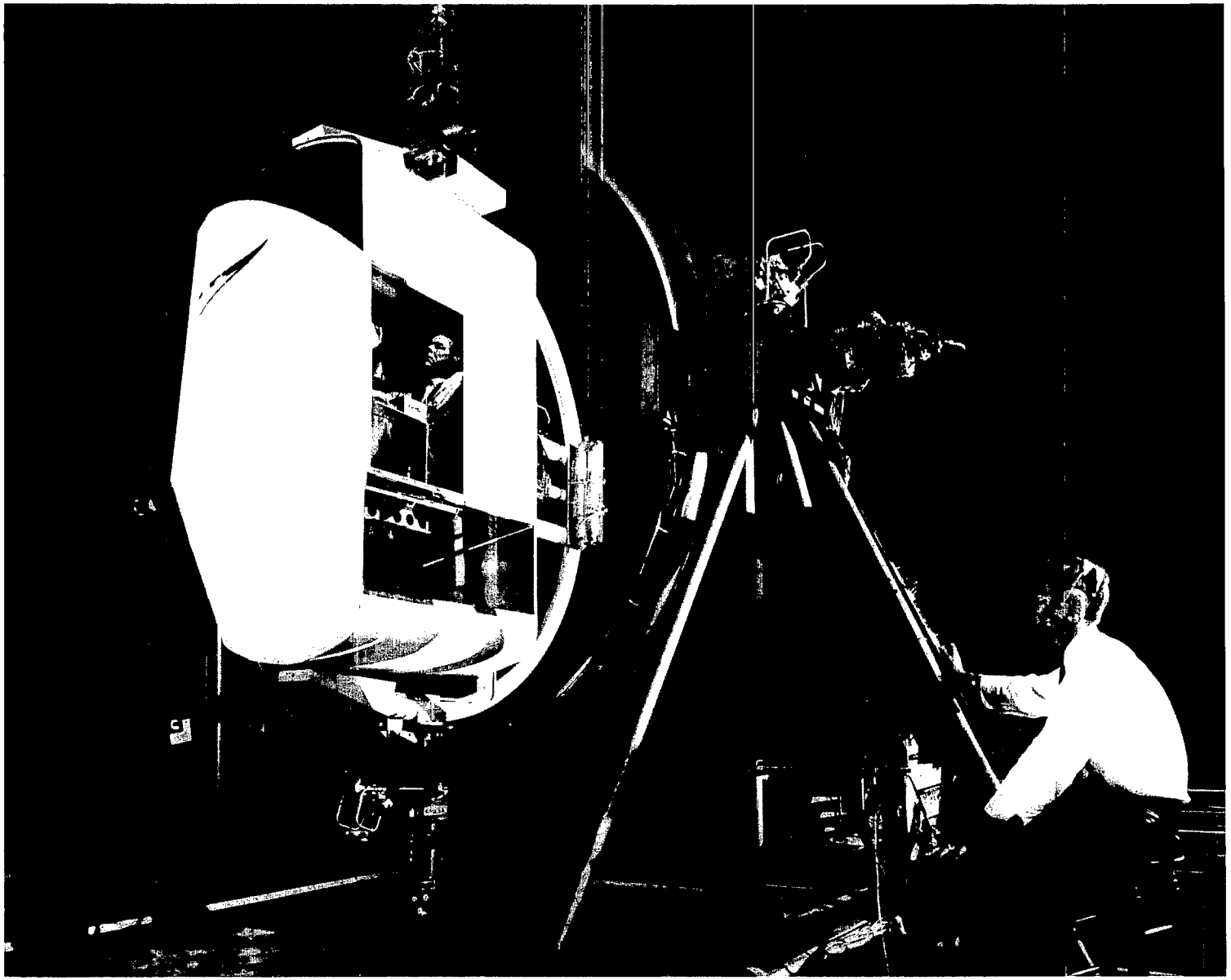

Figure 3.- Three-degree-of-freedom gimbal mounted simulator. L-62-5543

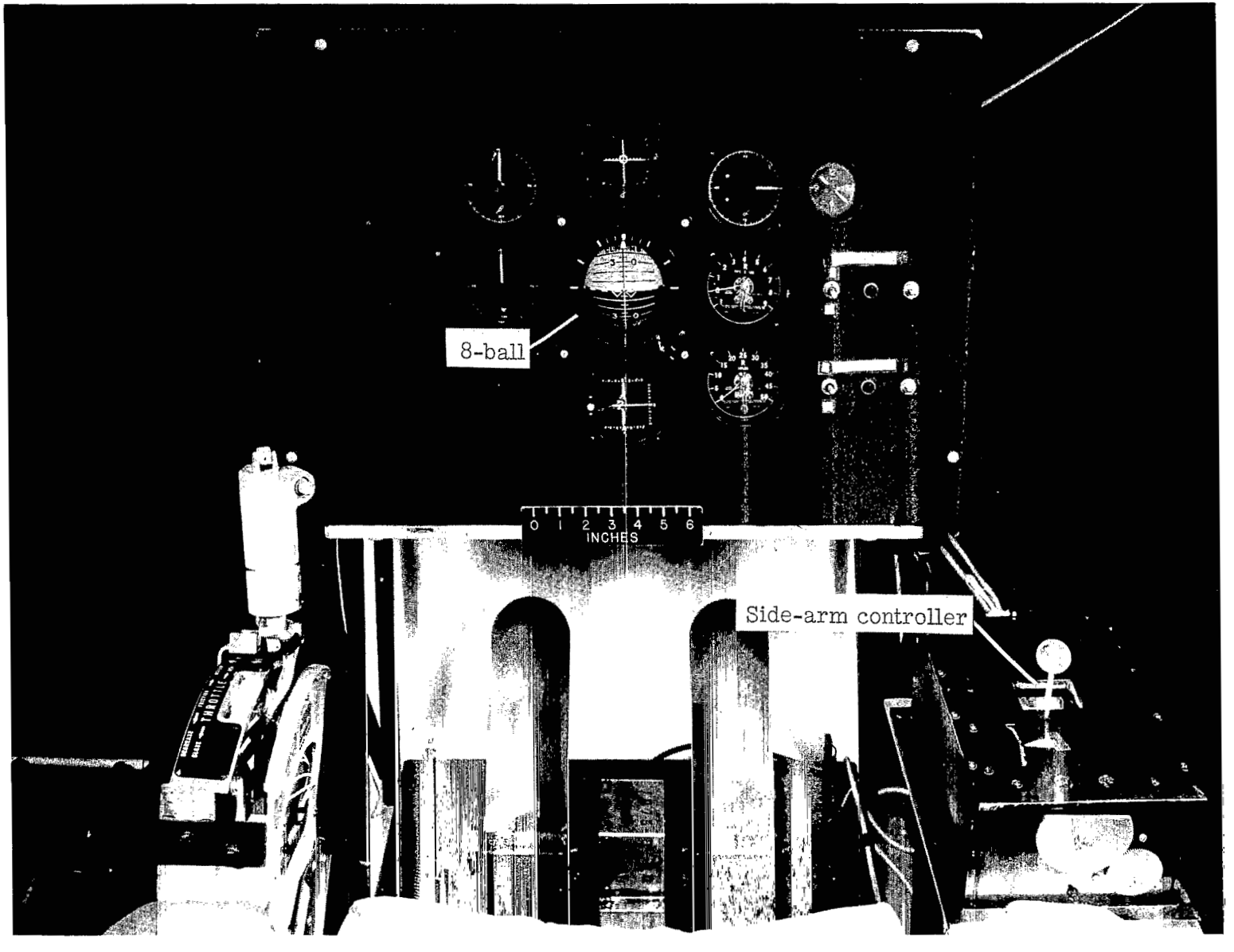

Figure 4.- Instrument panel. L-60-4266

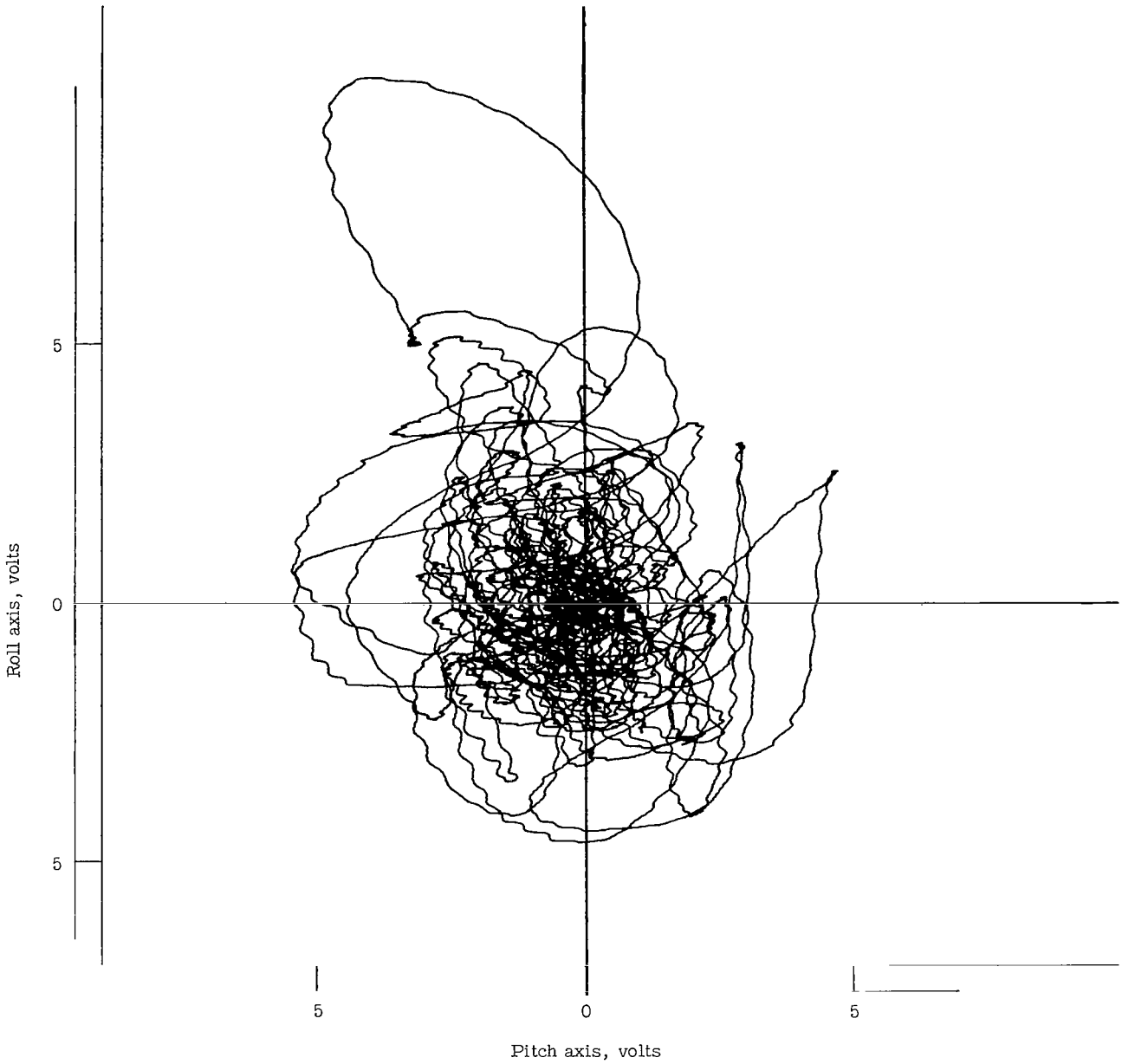

Figure 5.- X,Y plot of error from pitch and roll axes.

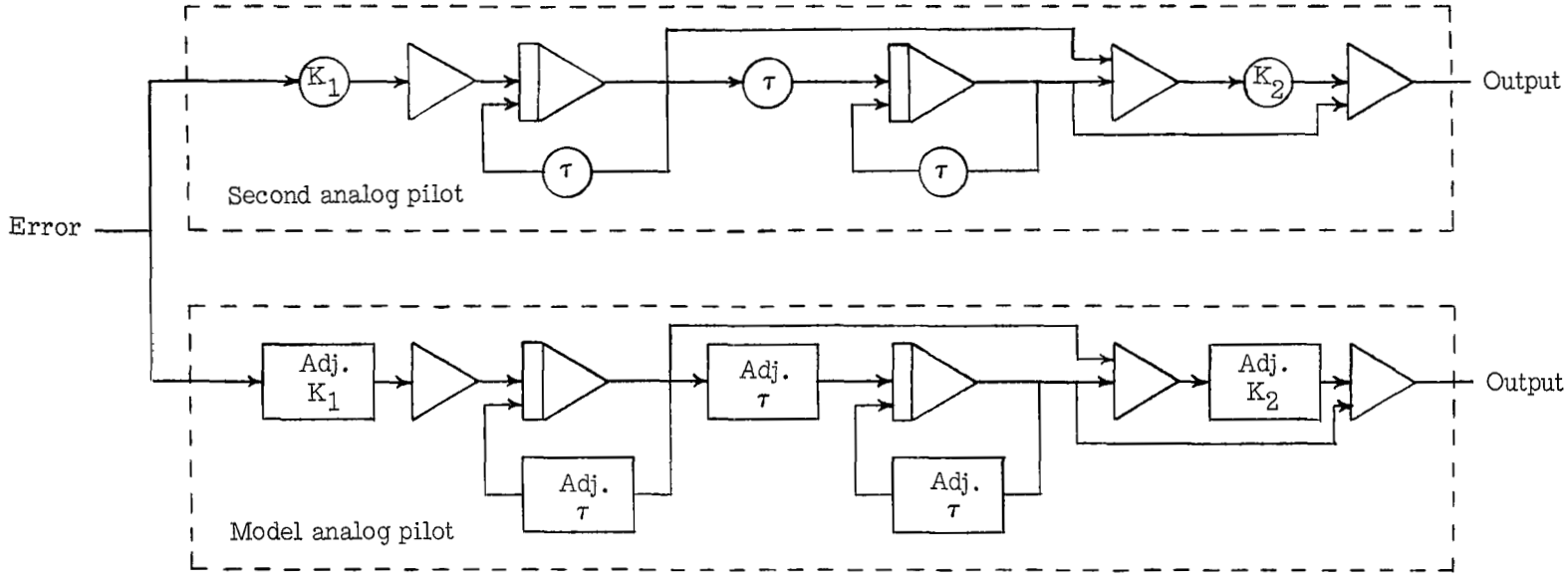

Figure 6.- Computer diagram of model analog pilot and fixed-gain analog pilot.

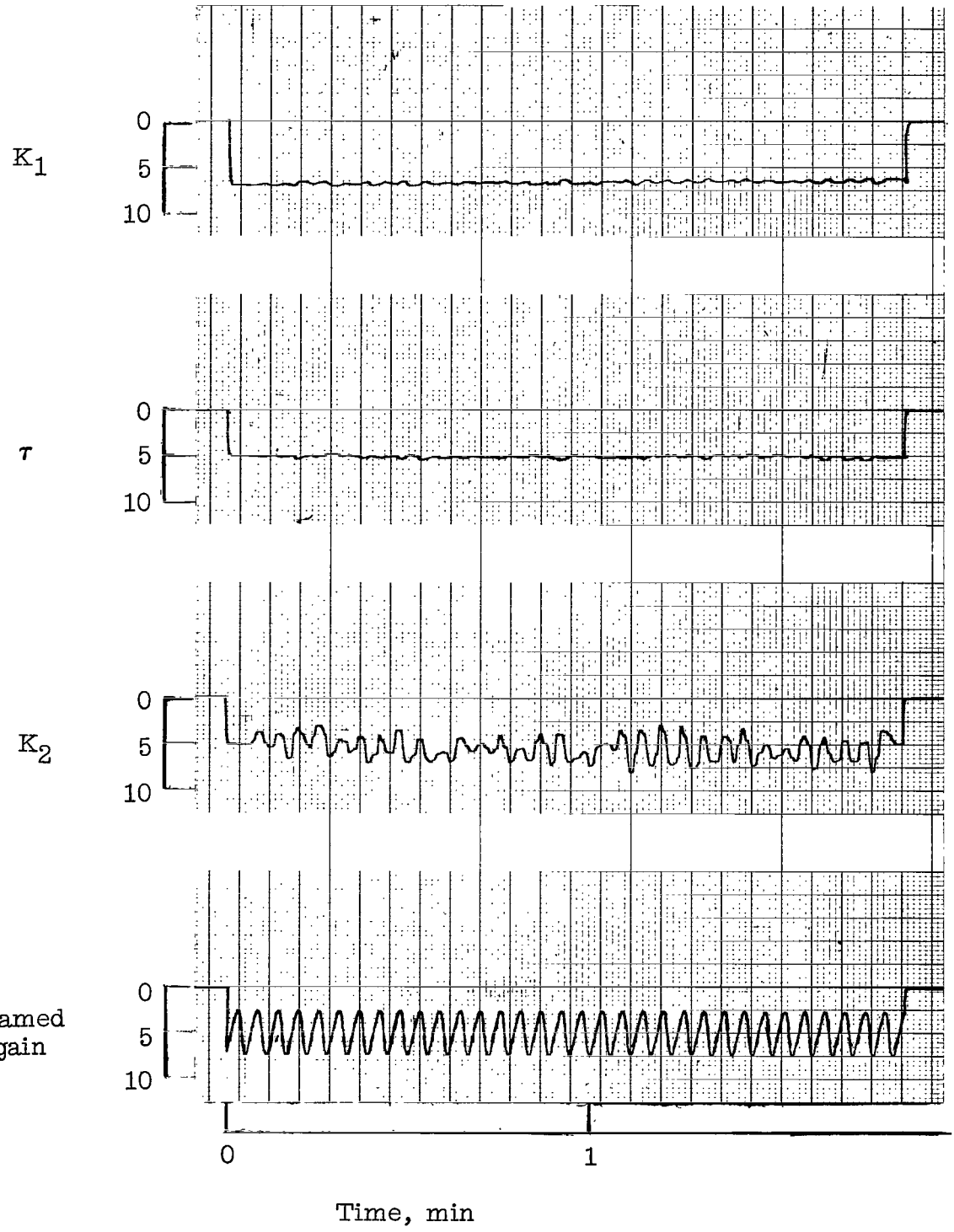

Figure 7.- Matching of a variable K_2 gain.

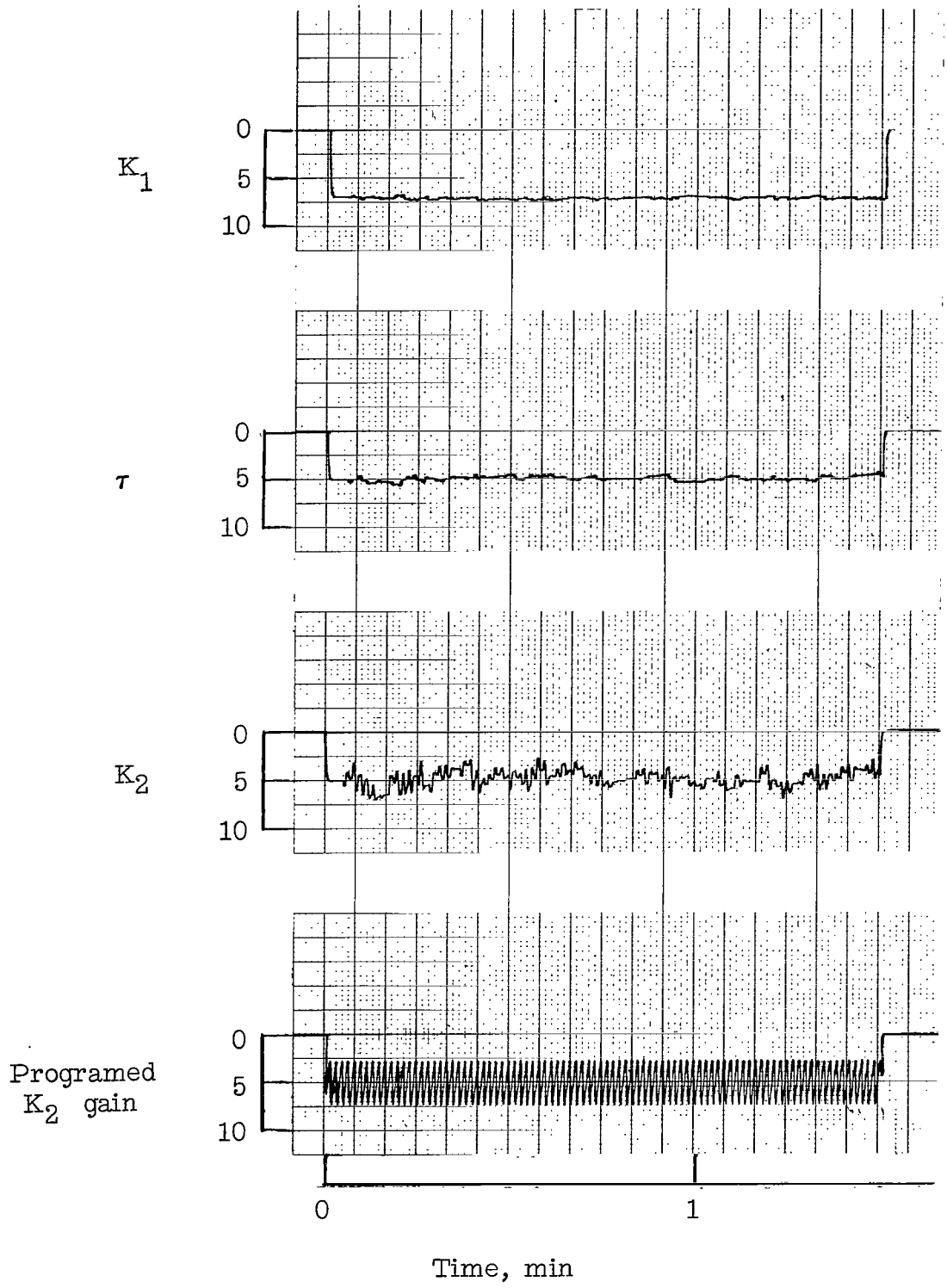

Figure 8.- Matching of a variable K_2 gain.

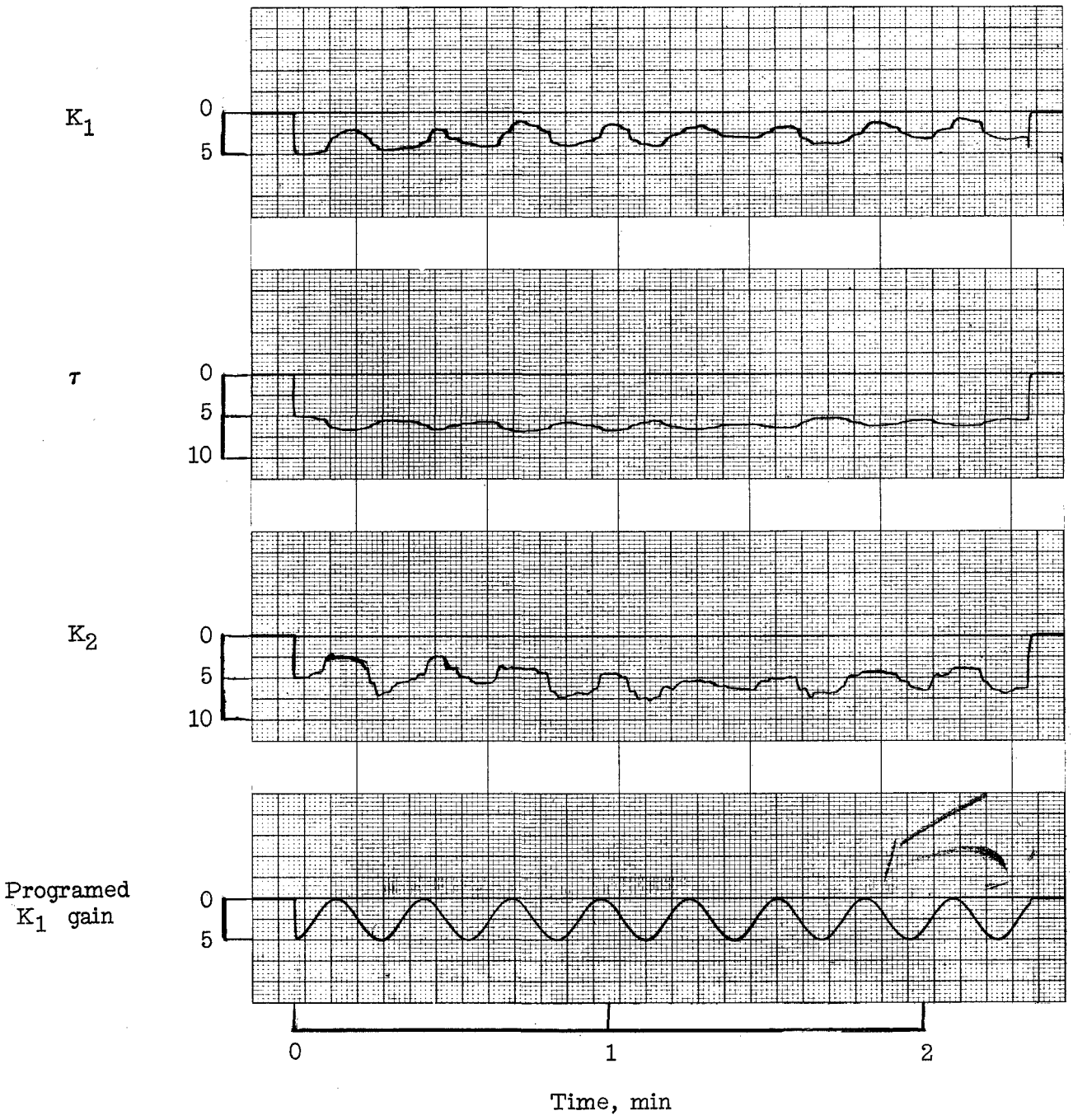

Figure 9.- Matching of a variable K_1 gain.

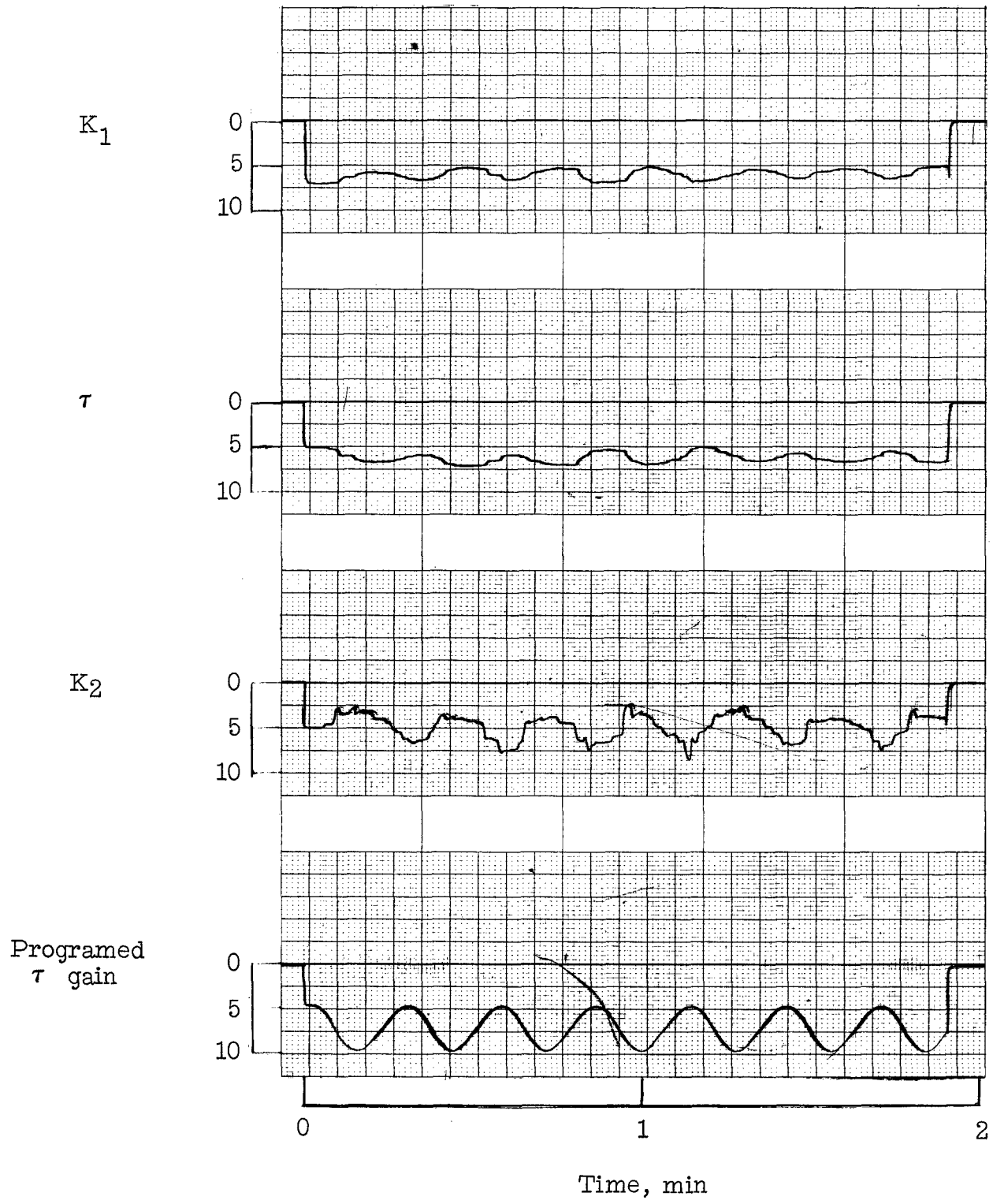

Figure 10.- Matching of a variable τ gain.

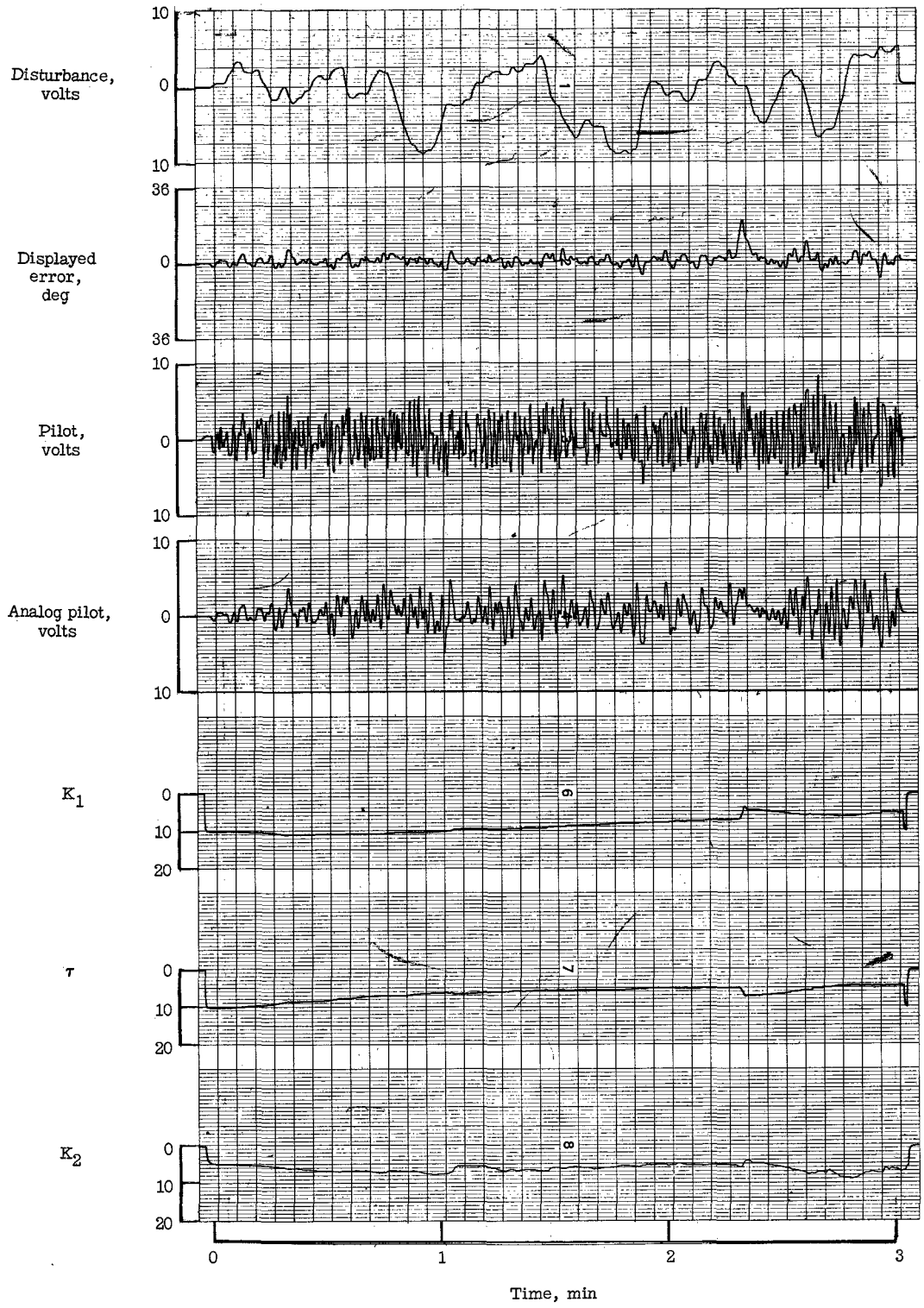

Figure 11.- Record of pilot A, single axis, no motion.

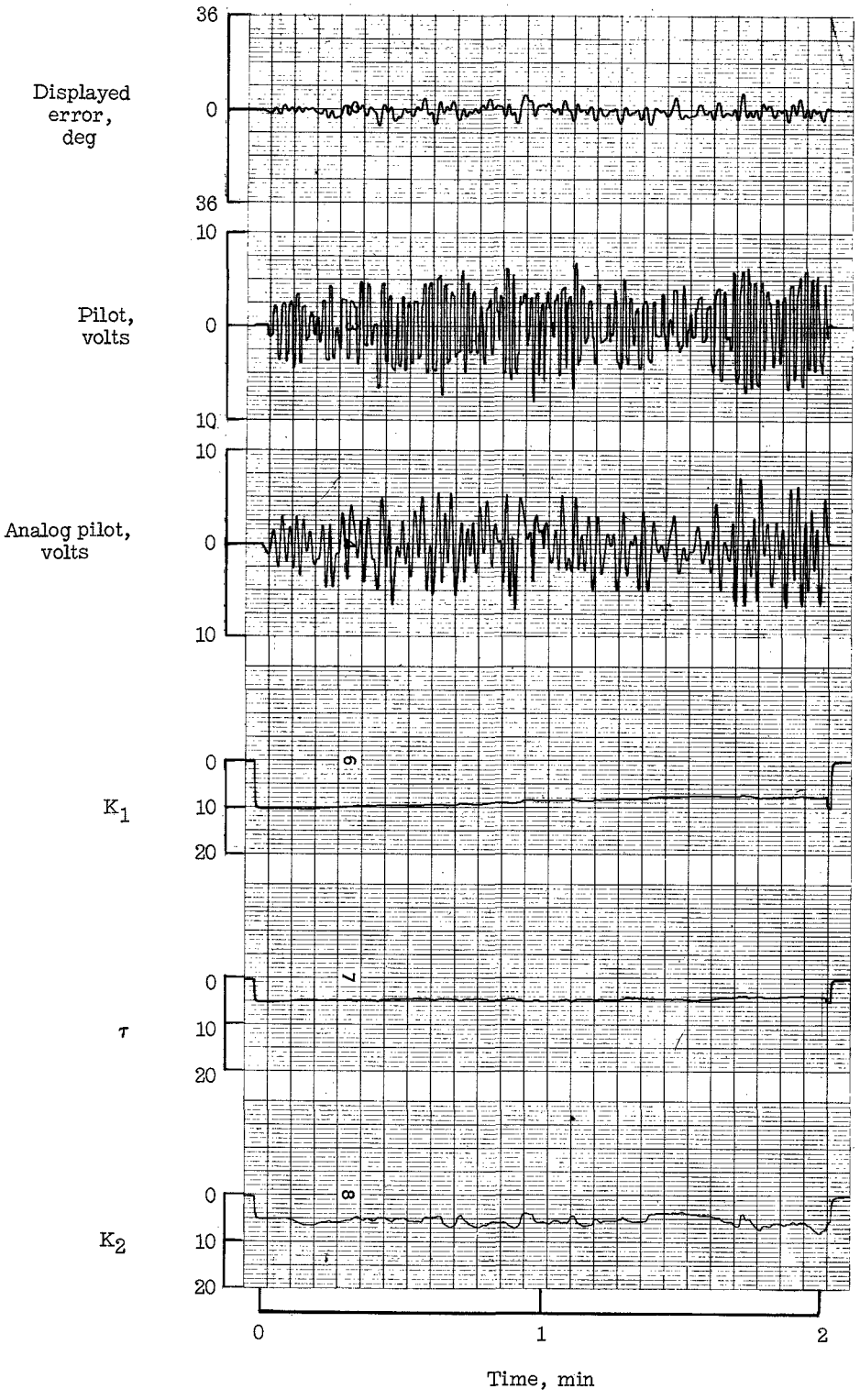

Figure 12.- Record of pilot B, single axis, no motion.

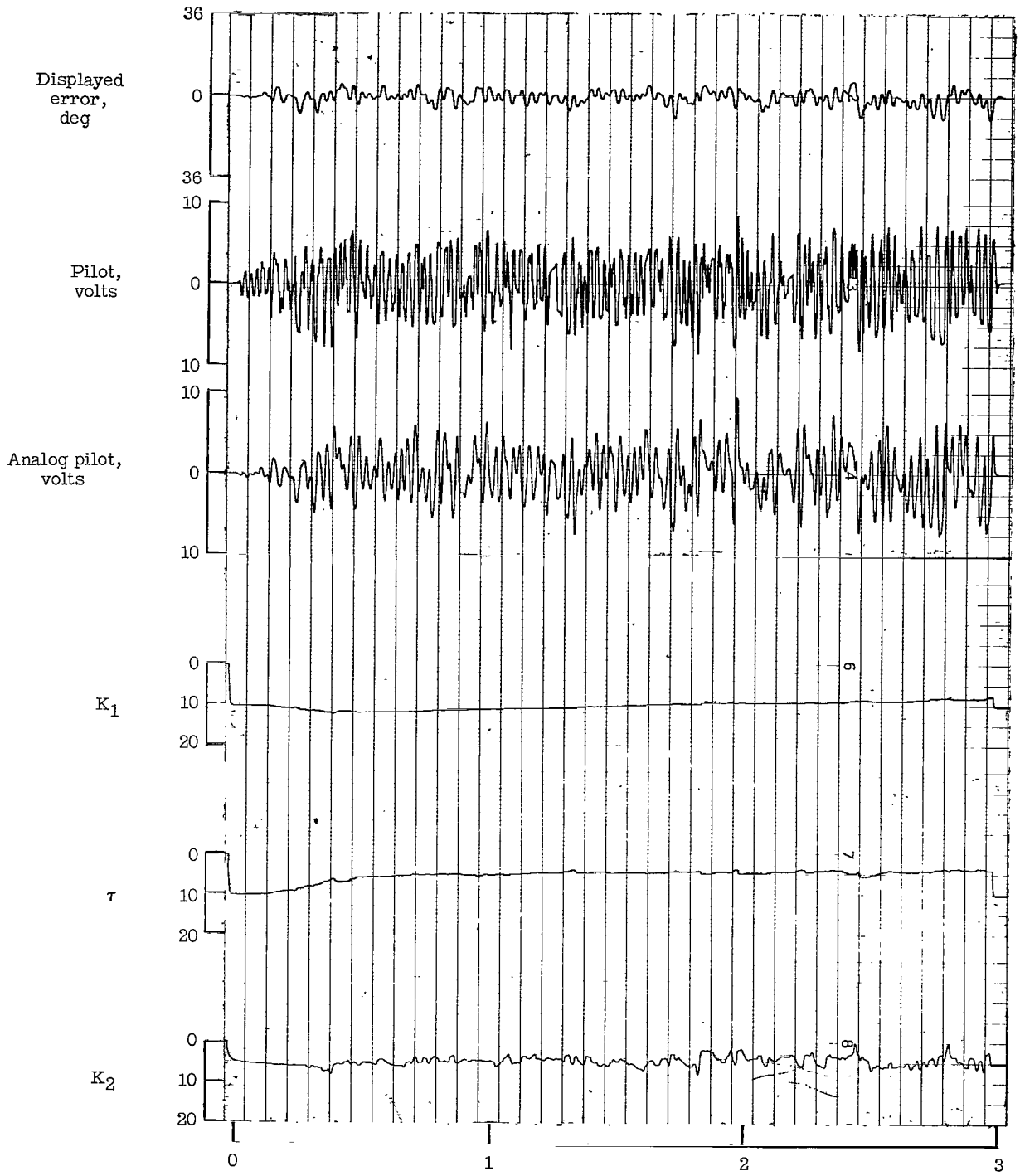

Figure 13.- Record of pilot D, single axis, no motion.

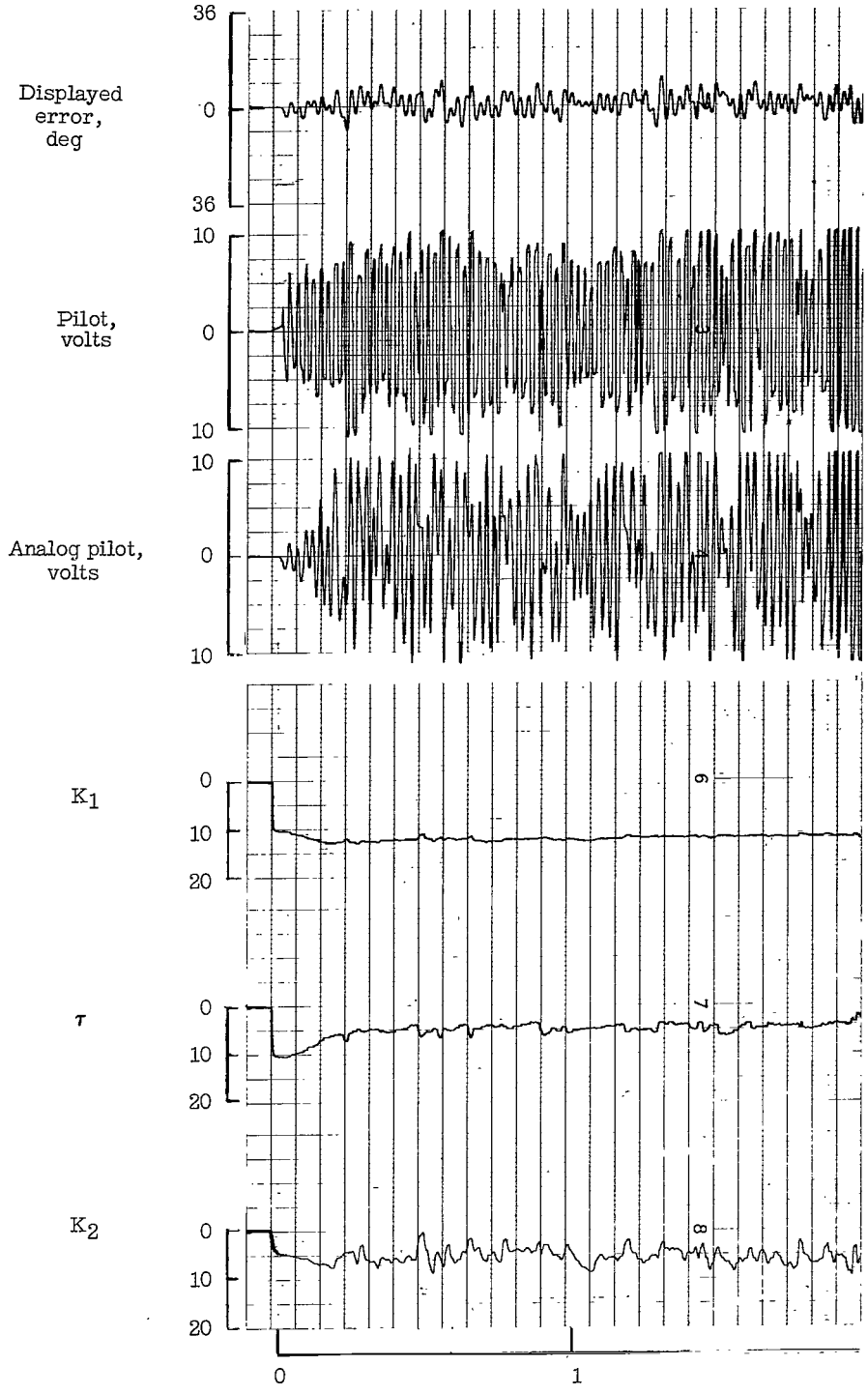

Figure 14.- Record of pilot A, single axis, with motion.

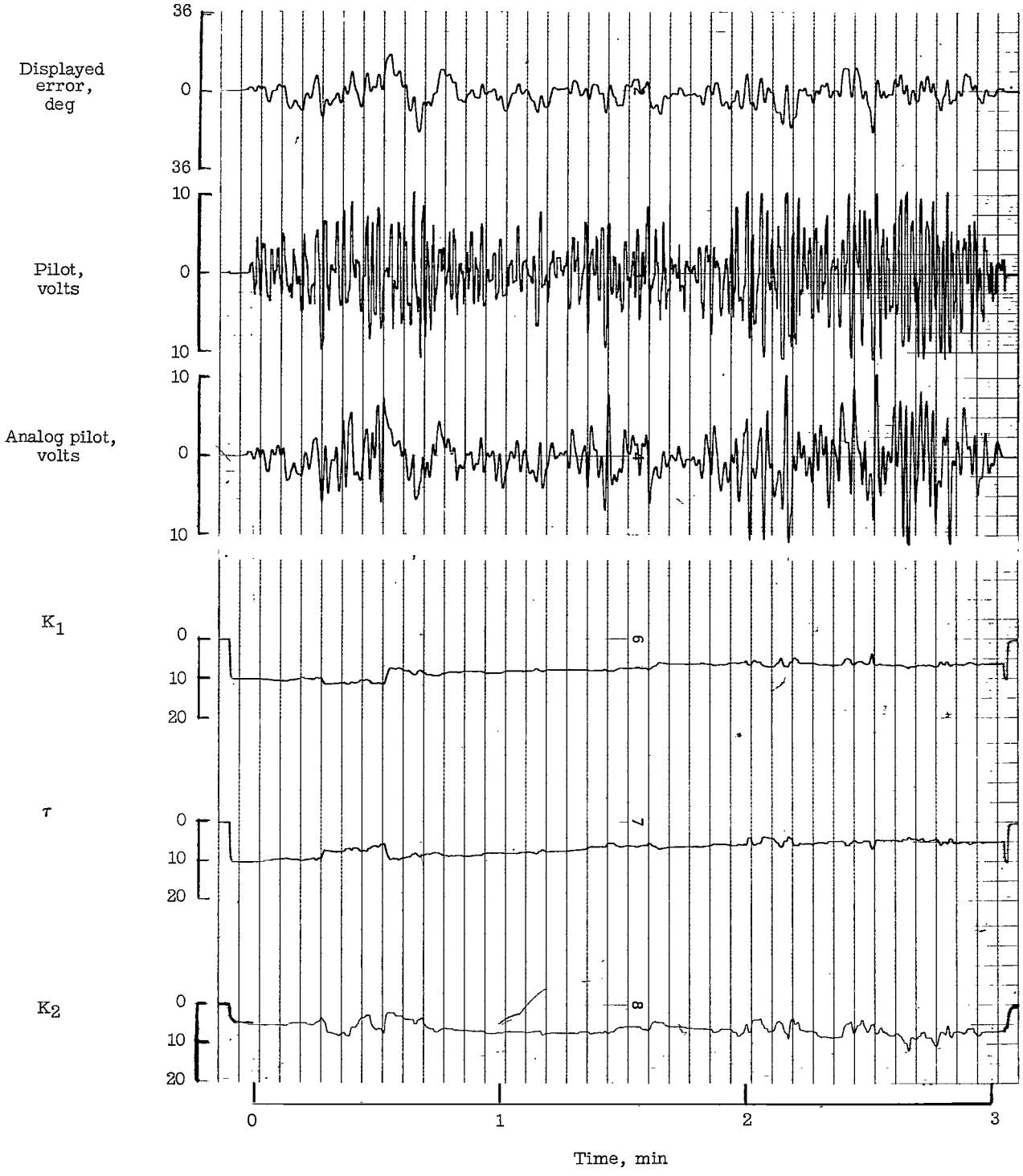

Figure 15.- Record of pilot A, first axis of 2, no motion.

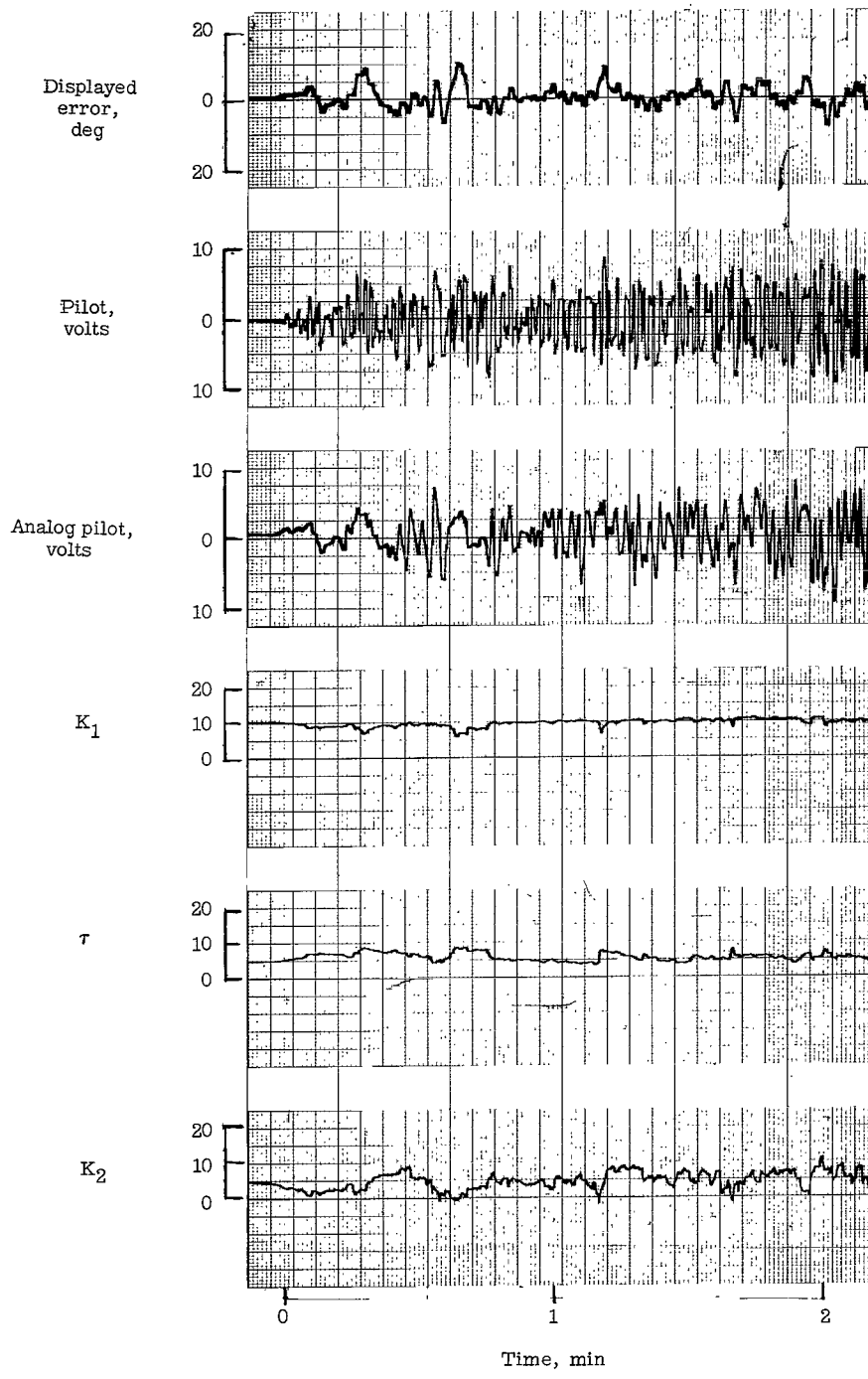

(a) Initial run.

Figure 16.- Record of pilot A, second axis of 2, no motion.

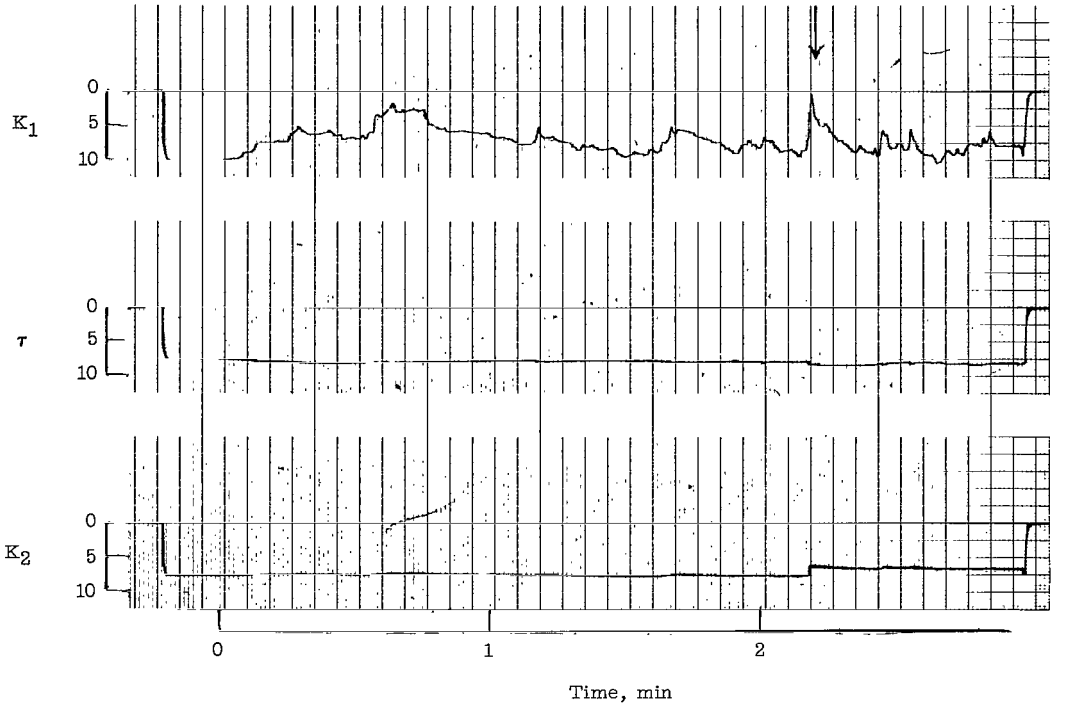

(b) Gain values with τ and K_2 gain variation kept to a minimum.

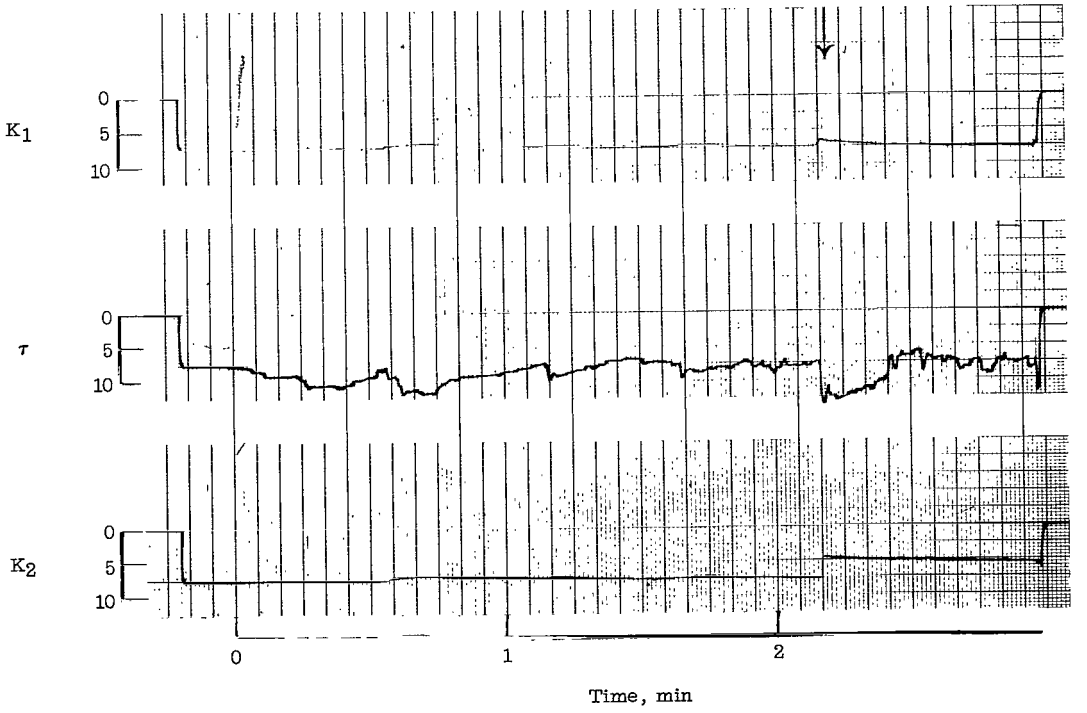

(c) Gain values with K_1 and K_2 gain variation kept to a minimum.

Figure 16.- Continued.

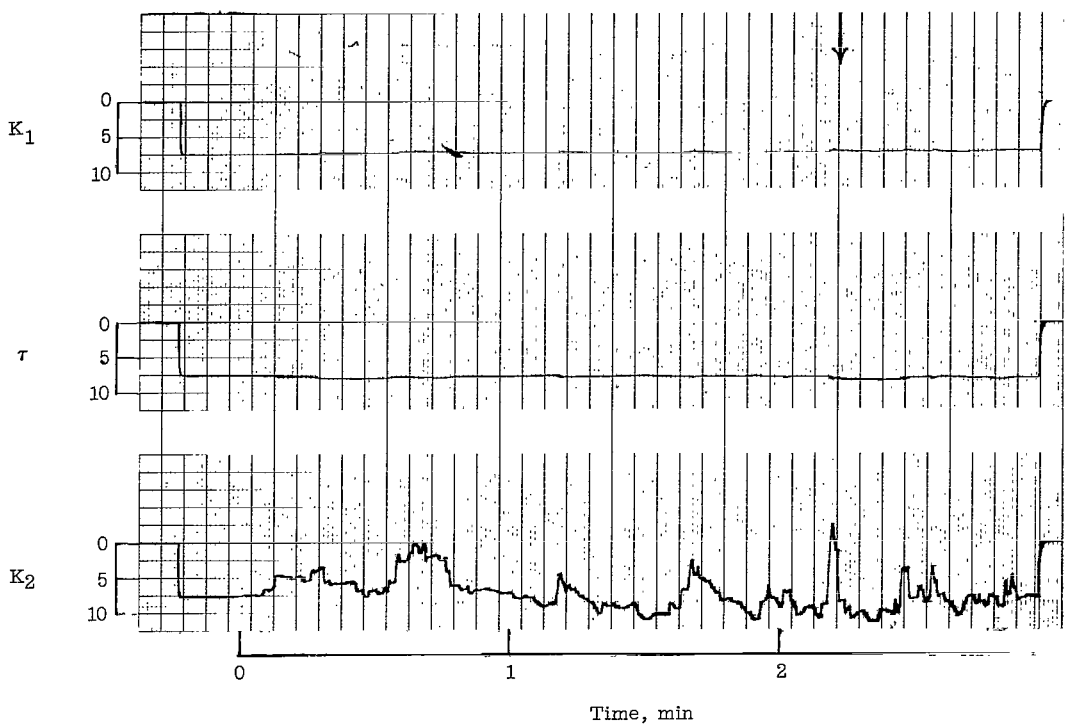

(d) Gain values with K_1 and τ gain variation kept to a minimum.

Figure 16.- Concluded.

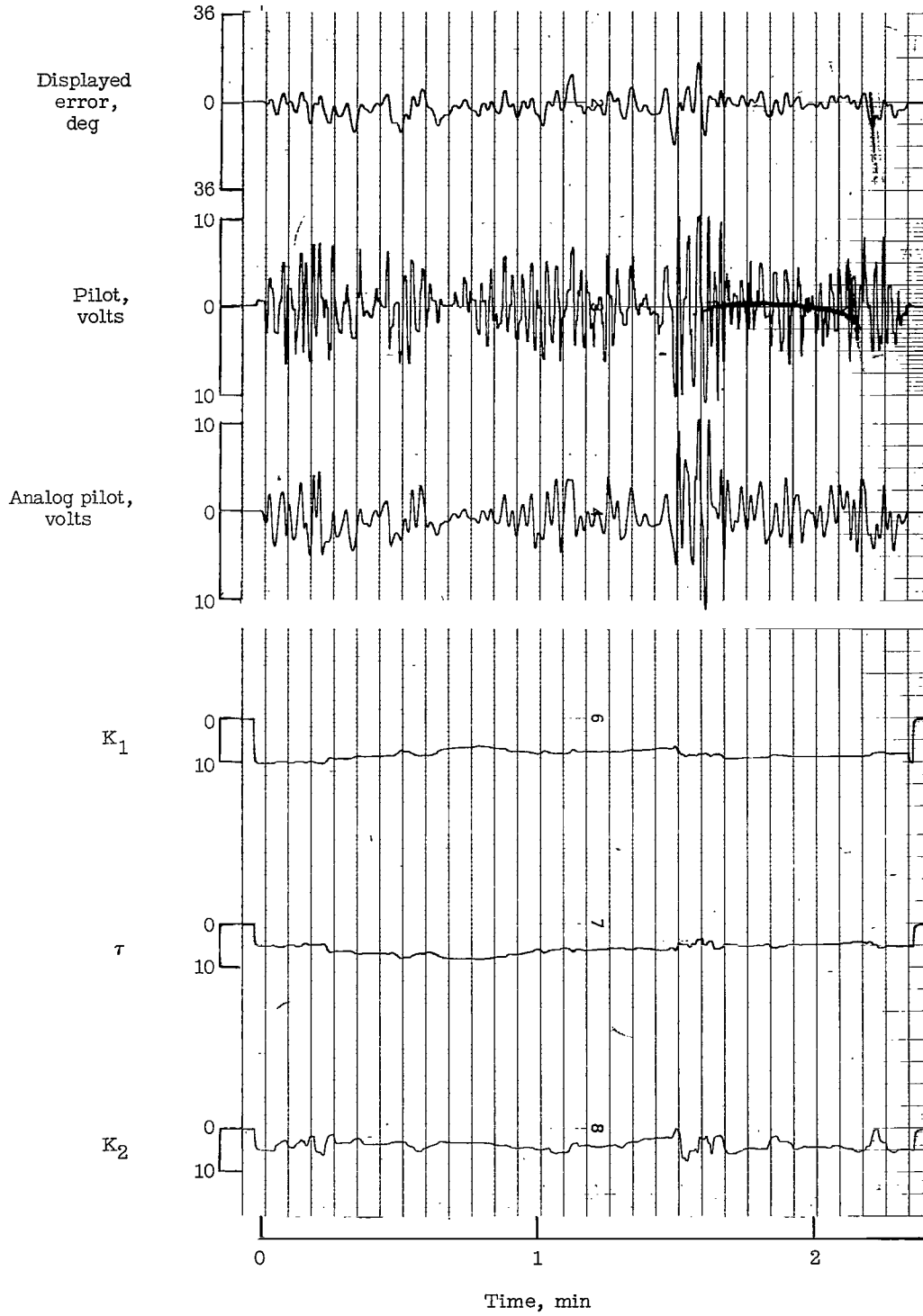

Figure 17.- Record of pilot B, first axis of 2, no motion.

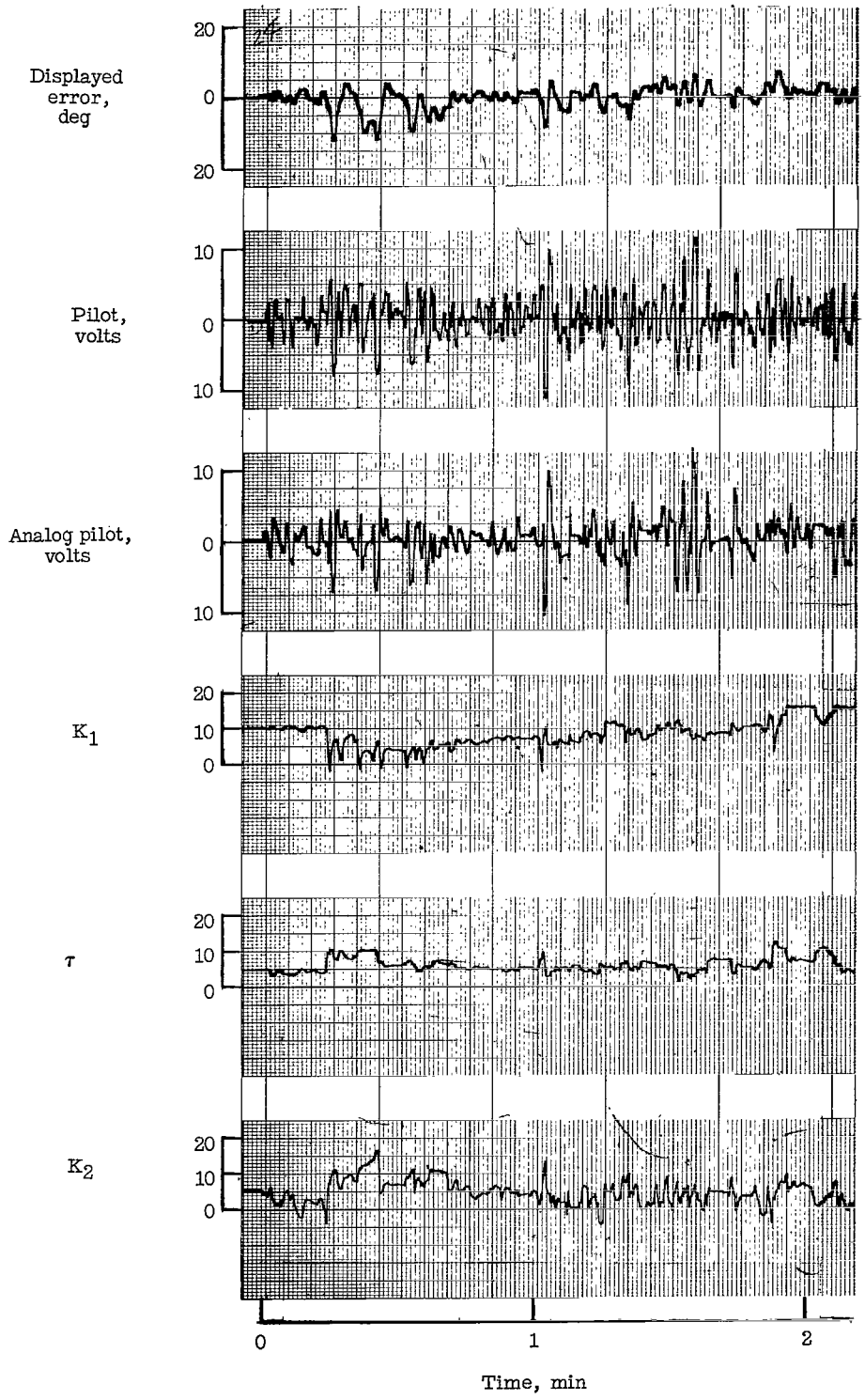

Figure 18.- Record of pilot B, second axis of 2, no motion.

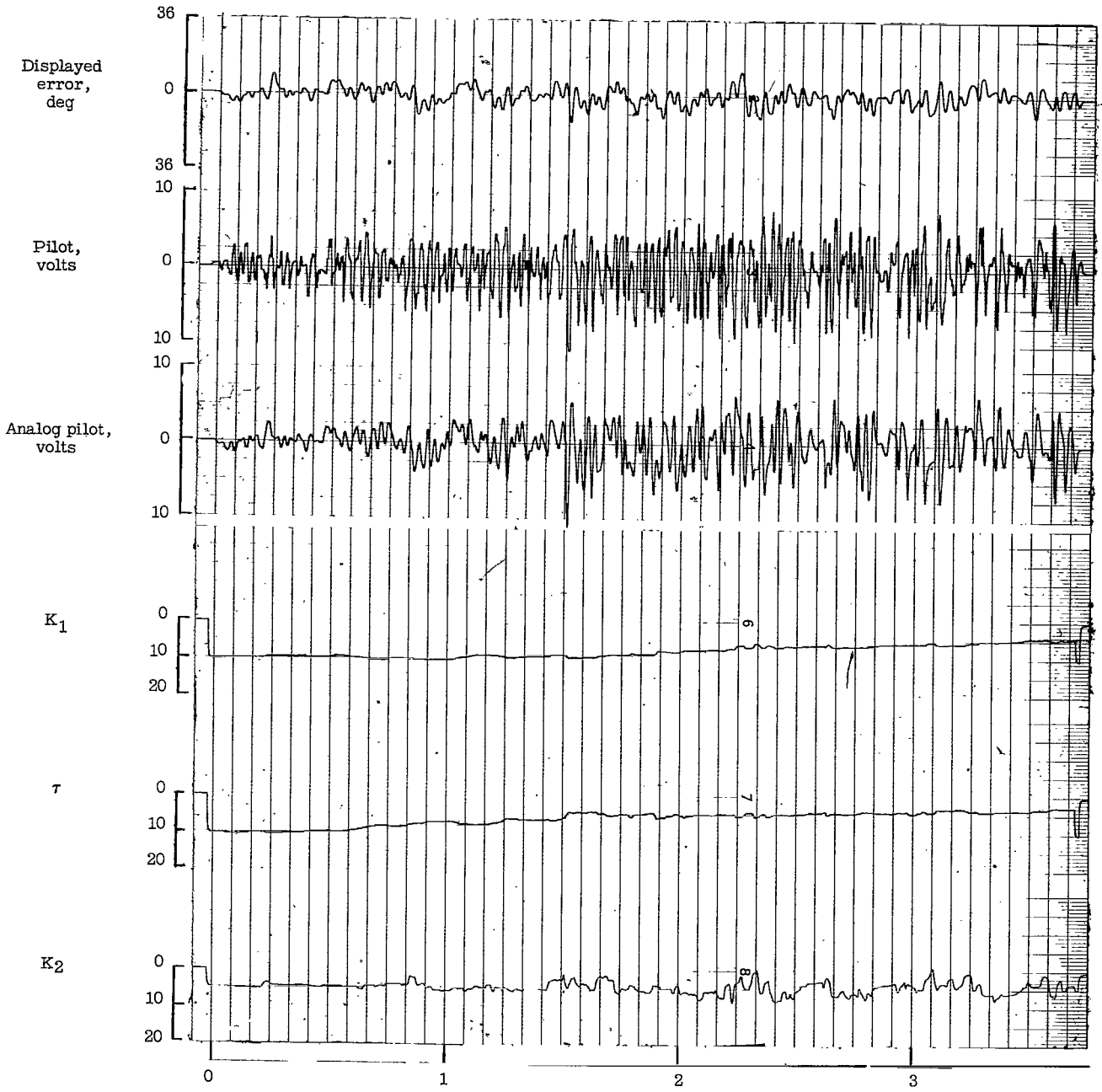

Figure 19.- Record of pilot D, first axis of 2, no motion.

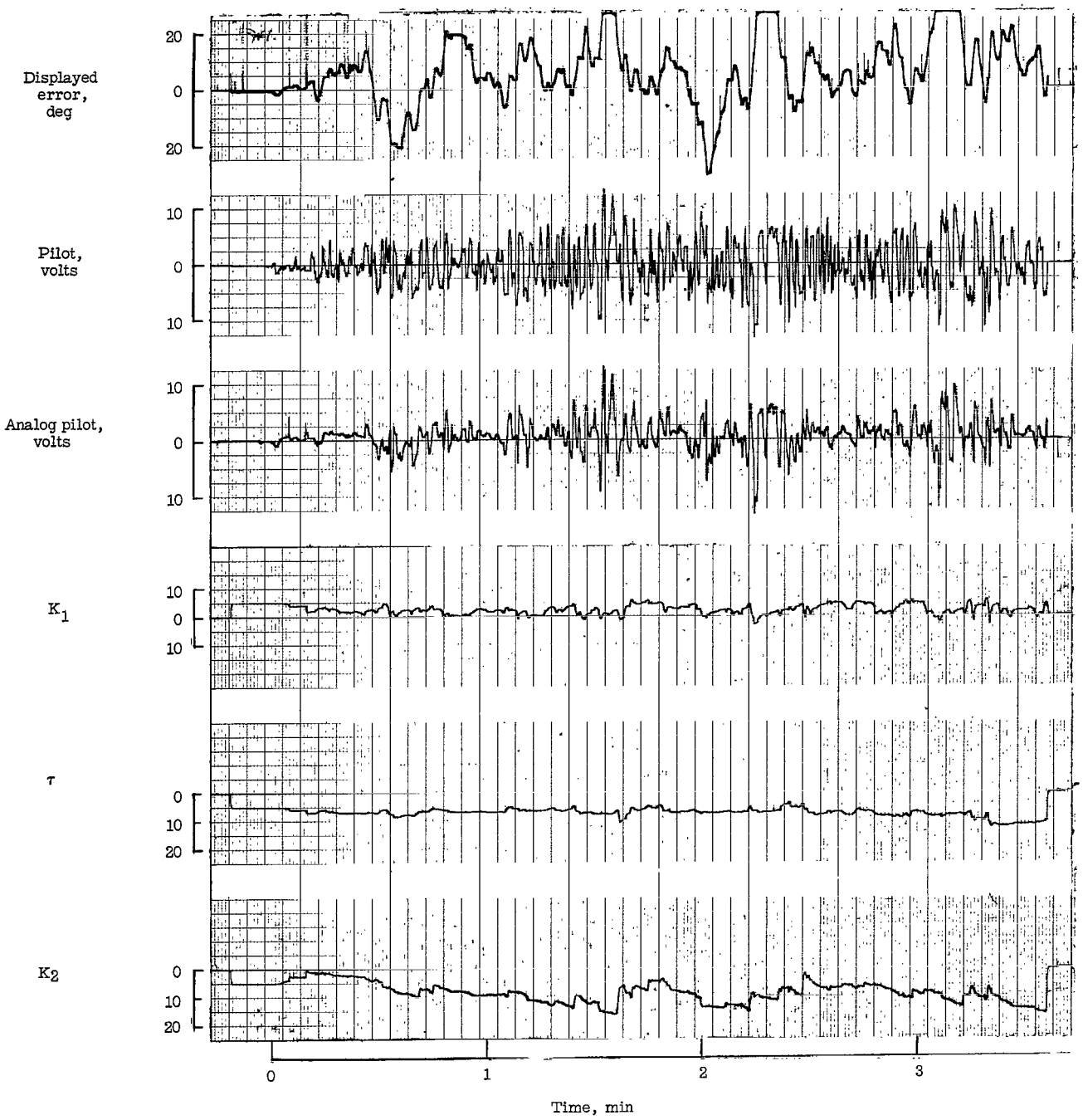

Figure 20.- Record of pilot D, second axis of 2, no motion.

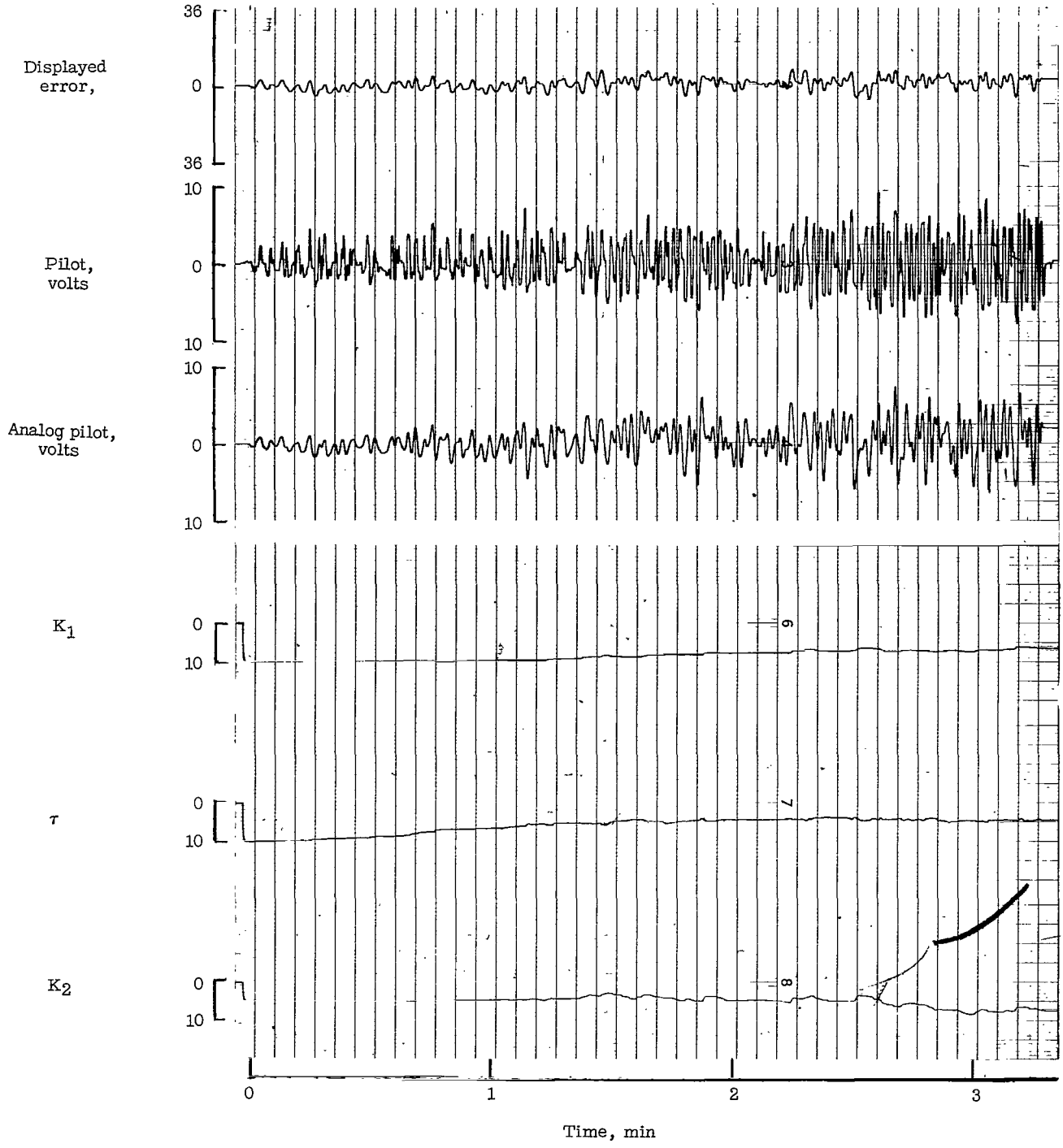

Figure 21.- Record of pilot A, first axis of 2, with motion.

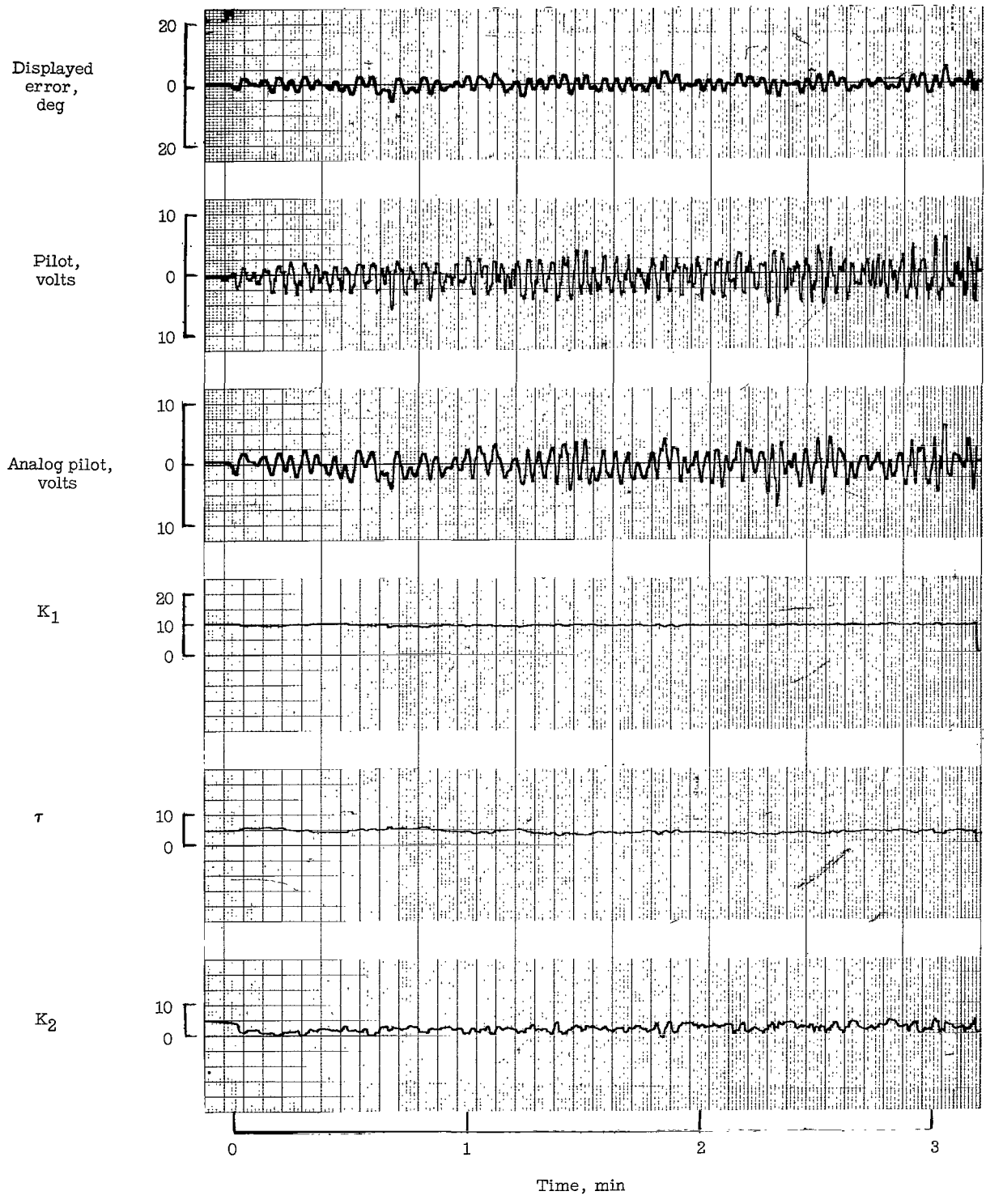

Figure 22.- Record of pilot A, second axis of 2, with motion.

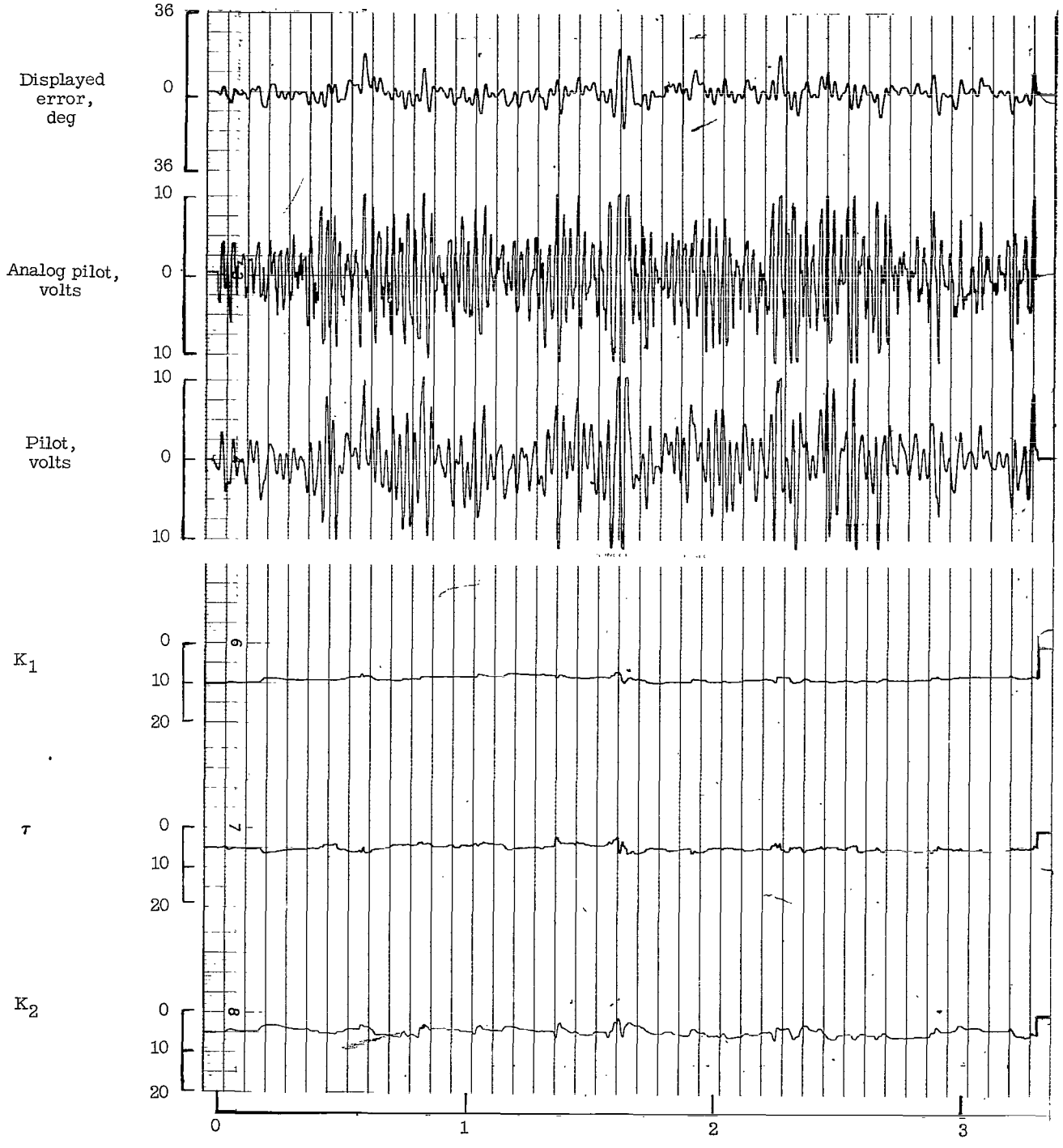

Figure 23.- Record of pilot B, first axis of 2, with motion.

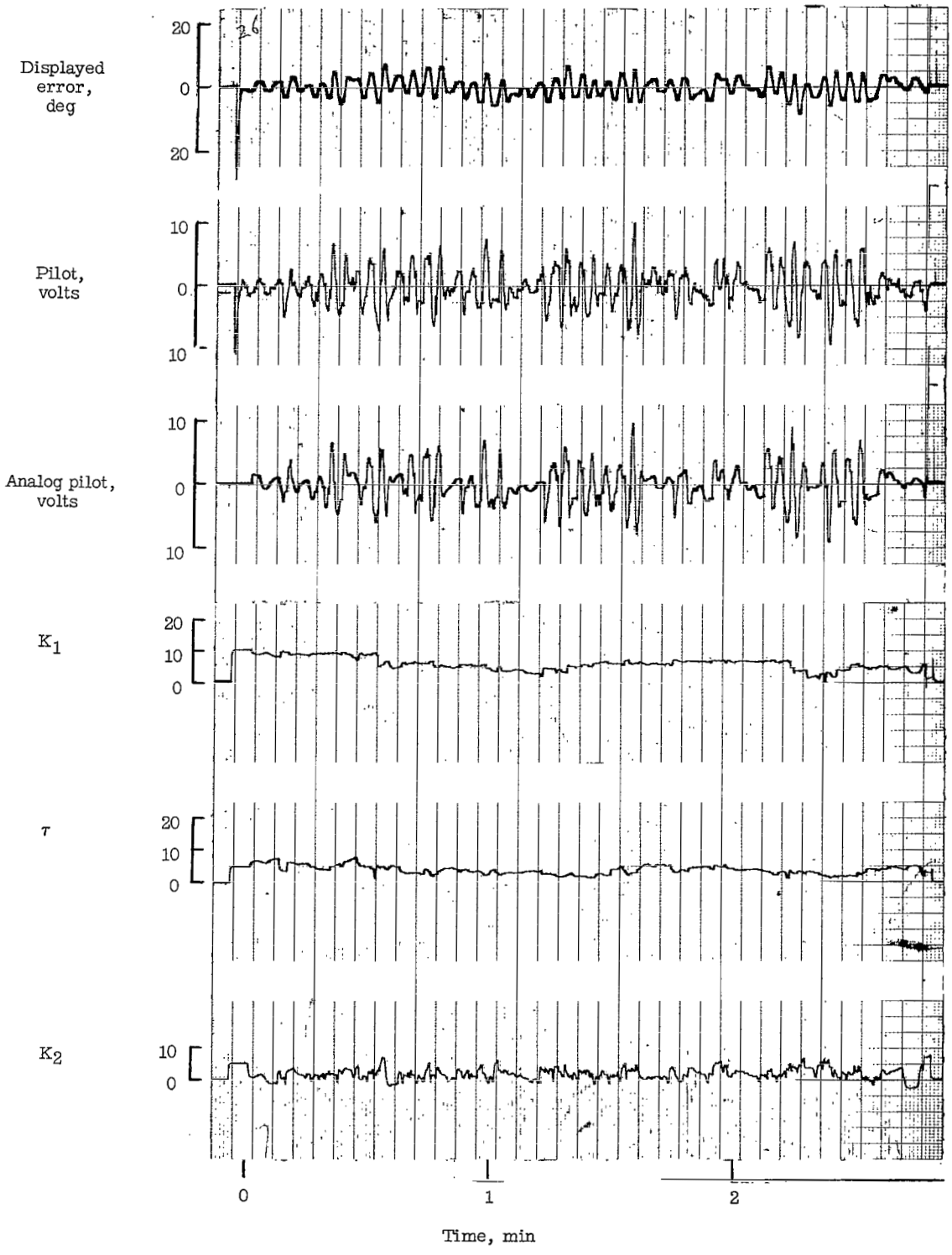

Figure 24.- Record of pilot B, second axis of 2, with motion.

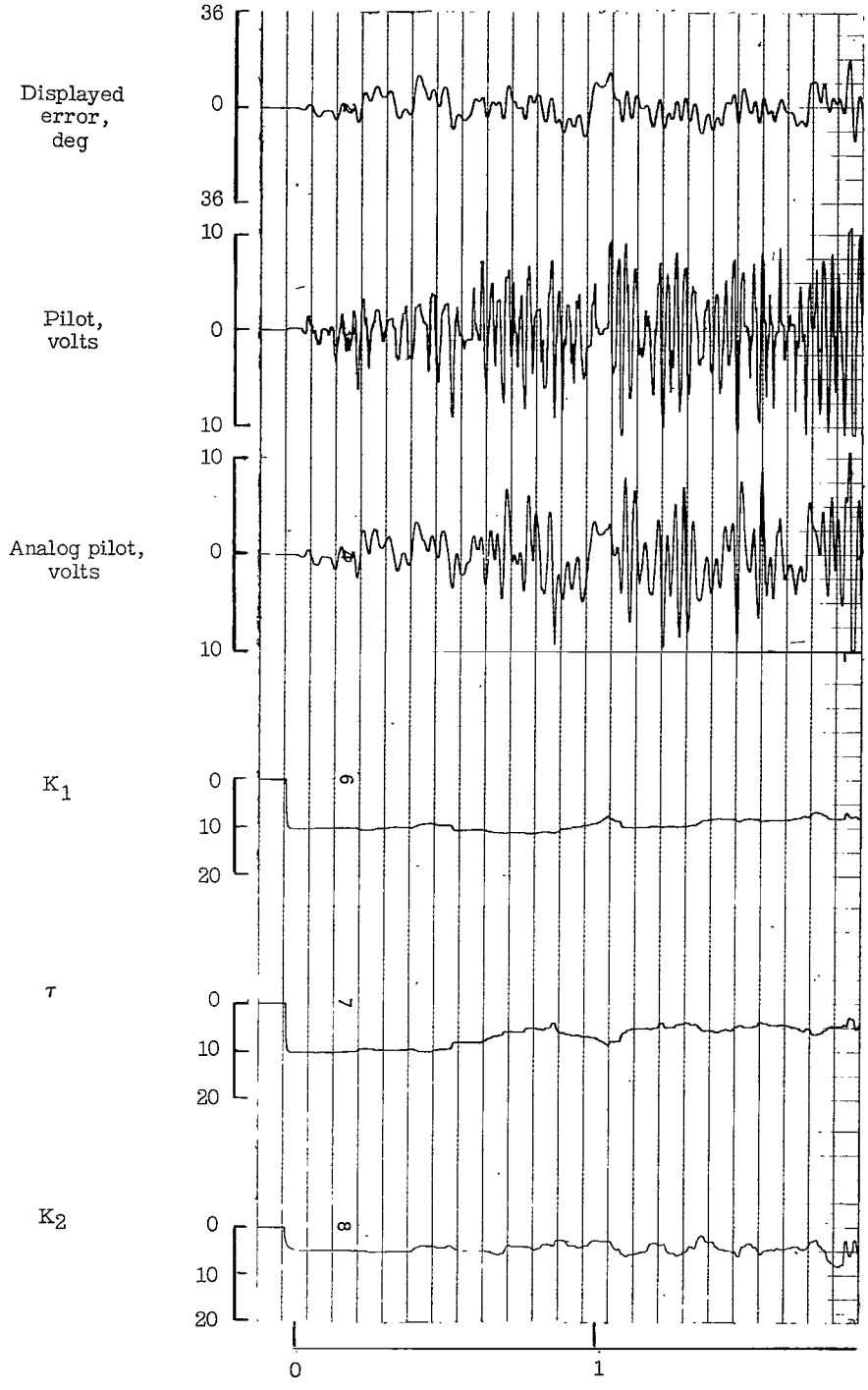

Figure 25.- Record of pilot D, first axis of 2, with motion.

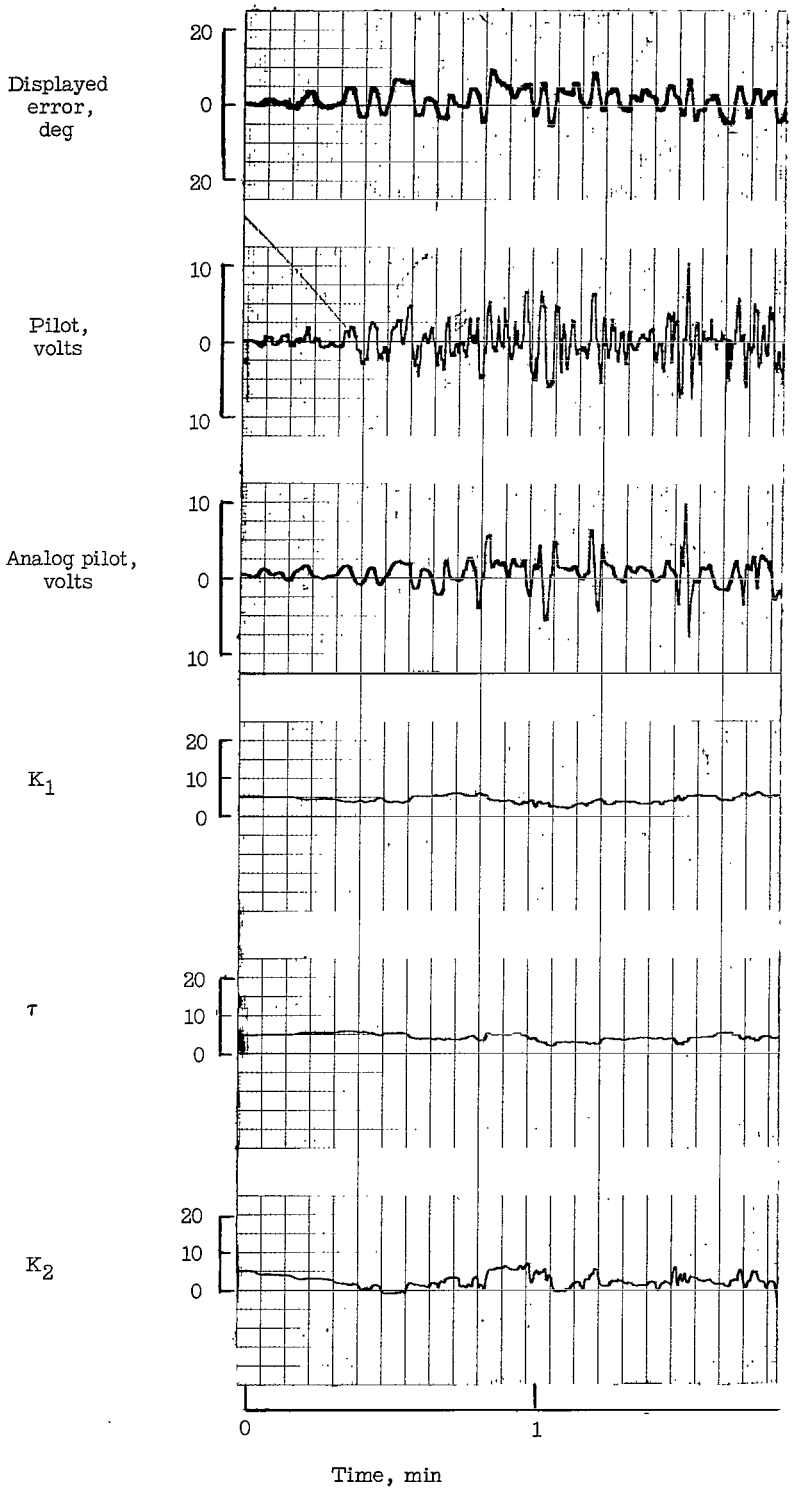

Figure 26.- Record of pilot D, second axis of 2, with motion.

2/7/85
ØS